Master's thesis

NTNU
Norwegian University of Science and Technology
Faculty of Natural Sciences
Department of Chemical Engineering

Jens Petter Flem

Opportunities of small-scale hydrogen production from MSWI fly ash

Master's thesis in Chemical Engineering and Biotechnology
Supervisor: Hanna Knuutila and Andressa Nakao
Co-supervisor: Haakon Rui
June 2022

NTNU
Norwegian University of Science and Technology

Jens Petter Flem

Opportunities of small-scale hydrogen production from MSWI fly ash

Master's thesis in Chemical Engineering and Biotechnology
Supervisor: Hanna Knuutila and Andressa Nakao
Co-supervisor: Haakon Rui
June 2022

Norwegian University of Science and Technology
Faculty of Natural Sciences
Department of Chemical Engineering

NTNU
Norwegian University of
Science and Technology

Abstract

This thesis presents a preliminary techno-economic assessment of opportunities for hydrogen production from MSWI fly ash. The thesis is in collaboration with the company NOAH, which operates the waste treatment plant where the production takes place. The thesis is a continuation of previous work on the topic and build upon the previous results and conclusions. The objective of this thesis is to investigate two main alternatives of application: purification of the hydrogen for usage in fuel cells and process heat production. Their practical and economical feasibility are investigated and compared.

The assumed hydrogen production at NOAH is 180 tons per year and 50 kg/h, which was deemed to little to sell. On-site applications were therefore investigated. Alternative 1: Fuel cells, describes a system for production, compression, purification, and storage of the hydrogen for further use in fuel cells. Alternative 2: Process heat production, describes a system for production and combustion of the gas in a boiler for stream production.

The quality of the purified hydrogen gas in Alternative 1 was not found to fulfill the required standard for use in proton-exchange membrane fuel cells, with use of the investigated purification method. The hydrogen content was found to be high enough and several of the impurities were complete removed in the purification. However, the content of carbon monoxide and water were found to be too high. Alternative 2 was found to produce a flue gas with a composition of 60% nitrogen, 37% water, 3% oxygen and trace amounts of other components, from the combustion of the hydrogen gas stream with air. The process heat production was found to be 1.54 MW, which gave a steam production of 2070 kg/h. This production could cover around 1/3 of NOAH's steam demand.

The total cost of Alternative 1 was estimated to be 2.81 MUSD without and 8.04 MUSD with installation. The hydrogen production cost for a ten year horizon was found to be 4.5 USD/kgH_2, which is comparable to values from the open literature. The total cost of Alternative 2 was estimated to 1.44 MUSD without and 3.48 MUSD with installation. The steam production cost was estimated to be 0.045 USD/kg steam over a ten year time period, which is significantly higher than values from the open literature.

Sammendrag

Denne avhandlingen presenterer en innledende tekno-økonomisk vurdering av mulighetene for hydrogenproduksjon fra MSWI flyveaske. Arbeidet har blitt utført i samarbeid med selskapet NOAH, som driver anlegget for avfallshåndtering hvor hydrogenproduksjonen forekommer. Avhandlingen er en videreføring av tidligere arbeid, og bygger på de tidligere resultatene og konklusjonene. Målet for denne avhandlingen er å undersøke to alternativer for bruk av hydrogenet: rensing av hydrogengassen for videre bruk i brenselceller og produksjon av prosessvarme. Den praktiske og økonomiske gjennomførbarheten til alternativene er undersøkt og sammenlignes.

Den antatte hydrogenproduksjonen hos NOAH er 180 tonn per år og 50 kg per time, som er ansett å være for lite til å selges. Muligheter for bruk av hydrogenet på produksjonsstedet ble derfor undersøkt. Alternativ 1: Brenselceller, beskriver et system for produksjon, kompresjon, rensing og lagring av hydrogenet for videre bruk i brenselceller. Alternativ 2: Produksjon av prosessvarme, beskriver et system for produksjon og forbrenning av hydrogengassen med luft i en dampkjele for produksjon av damp.

Kvaliteten til den rensede hydrogengassen i Alternativ 1 ble ikke funnet til å være av den krevde standarden for bruk i proton-utveksling membran brenselceller, ved bruk av den undersøkte rensemetoden. Hydrogeninnholdet ble funnet til å være høyt nok og flere av urenhetene var fullstendig fjernet gjennom renseprosessen. Innholdet av karbonmonoksid og vann var derimot for høyt. Alternativ 2 produserer en røykgass med en sammensetning av 60% nitrogen, 37% vann, 3% oksygen og spormengder av andre komponenter. Produksjonen av prosessvarme var funnet til å være 1,54 MW, som ga en dampproduksjon på 2070 kg per time. Denne produksjonen kan dekke rundt en tredjedel av dampbehovet til NOAH.

Den totale kostnaden for Alternativ 1 ble estimert til 2,81 MUSD uten og 8,04 MUSD med installasjon. Produksjonskostnaden for hydrogen over en ti år lang horisont ble estimert til 4,5 USD per kg hydrogen, som er sammenlignbart med verdier fra den åpne litteraturen. Den totale kostnaden til Alternativ 2 ble estimert til 1,44 MUSD uten og 3,48 MUSD med installasjon. Produksjonskostnaden for damp ble estimert til 0,045 USD per kg damp over en periode på ti år. Denne verdien er betydelig høyere enn verdier fra den åpne litteraturen.

Acknowledgements

I want to express my gratitude to my supervisors Hanna Knuutila and Andressa Nakao for all the help and support they have given me throughout the last year. We have had many good discussions and it has been a pleasure to work with them.

As this thesis was written in cooperation with NOAH, I would like to thank both NOAH and my supervisor from the company Haakon Rui. He has been very helpful by answering all my questions as well as he could throughout both the specialization project and this Master's thesis. He has also been very supportive and given me the belief that my work this last year has been helpful and appreciated by the company. This has given additional motivation for working with the project.

Contents

Chapter 1

Introduction

The versatile energy carrier hydrogen, is a topic of growing interest in the energy sector [1] and is believed to be an important part of the current shift to sustainable energy [2]. Global warming is a major problem and a drastic reduction of greenhouse gas emissions are required in the years to come. The addition of an increasing global energy demand and diminishing fossil fuels, highlights the importance of a move to efficient, renewable energy sources. The shift to renewable energy sources are already underway, and new and improved technologies are under development. Energy from renewable sources can cover around 2/3 of the global energy demand and can therefore help substantially with the reduction of greenhouse gas (GHG) emissions [3]. This is essential for reaching the long-term goal of the Paris Agreement of keeping the temperature increase below 2 °C, and preferably below 1.5 °C [4].

A great reduction in greenhouse gas emissions is therefore essential in the near future. Hydrogen is a strong alternative for being a possible replacement of fossil fuels. It is described as one of the most important environmentally friendly and clean energy carriers which can be produced from renewable sources [5] [6]. Hydrogen has the potential to be a source for energy without emission of greenhouse gases [7]. It has very high energy density based on mass, in addition to a general low production cost and low carbon content [8], which are good characteristics for a potentially important part of future of the energy sector. The use of hydrogen in fuel cells for electricity production is very efficient with a high energy yield, while also being clean with no emission of CO_2 [5] [1].

The development of new technologies and innovations are required to achieve the mitigation of carbon dioxide emissions. This is especially important for the transportation sector, which to a great extent still is ignored in the international debate[3]. The transport sector is one of the major contributors to the high energy consumption and GHG emission. Hydrogen has real potential for being a solution for this sector. Hydrogen vehicles, both personal and heavy, are already in place, but they are not in use at a large scale yet. The high energy content and availability of hydrogen provides a good alternative fuel, but it's low energy density based on volume provide issues related to storage as high pressure is required. The hydrogen production and usage are still under development to become more competitive with the current alternatives. Several types of fuel cells are already developed for utilization of hydrogen, with PEM fuel cells being the dominant technology for hydrogen vehicles[9].

The hydrogen demand for all applications are expected to increase in the following years, mainly for energy and fuel cell utilization, while the cost for this sector is expected to decrease[10]. According to Arregi et al. (2018)[6], most of the current hydrogen production is used in ammonia production, while oil refining and methanol production also are significant application areas. Only around 8% was in 2018 used for other applications including energy production.

The increasing hydrogen demand is shown in Figure 1.1.

The production of today's hydrogen primarily comes from fossil energy sources. Steam methane reforming is the most dominant, while less carbon intensive methods also are in use. The most notable is electrolysis using electricity of low-carbon production. Gas reforming with carbon capture and storage is another alternative[10]. Hydrogen rich waste streams from the industry are also mentioned as alternative sources for hydrogen which could gain attraction in the future[1].

1.1 Case

The work in this thesis is a continuation of the previous work of a summer job and a specialization project[12]. This previous work is investigated further in this thesis, and the work is done in cooperation with the company NOAH.

NOAH is a company that works with processing and treatment of waste from both consumers and industrial production. The company processes

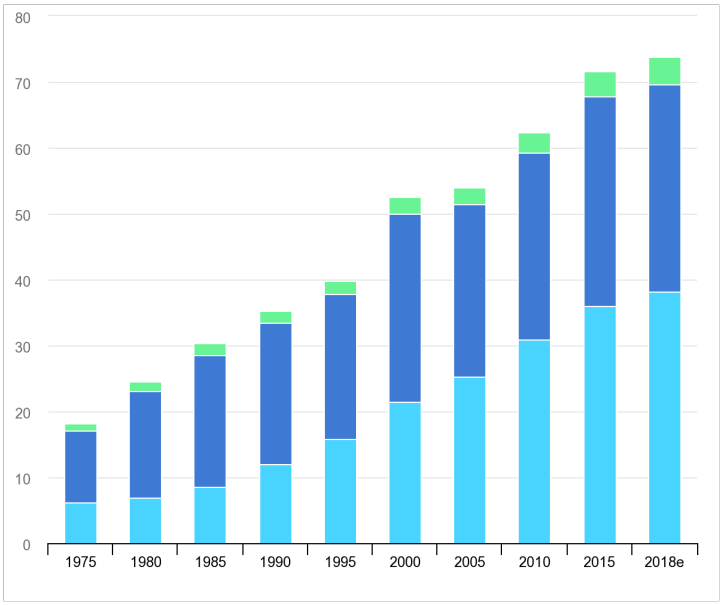

Figure 1.1: Global demand for pure hydrogen from 1975 to 2018 [11]. The colors indicate the application of the hydrogen: light blue indicates refining, dark blue indicates ammonia and green indicates other uses. The demand is given in megatons.

hazardous waste of varying contamination, and are in addition involved with clean-up of contaminated land and sea areas. Their plant involving treatment of inorganic hazardous waste is located on the island of Langøya off of Holmestrand south of Oslo. NOAH does also have a waste disposal site for inert waste and lightly contaminated excavation waste in Nittedal [13].

The project of this thesis focuses on the waste received at Langøya which contains fly ash from municipal solid waste incineration (MSWI) using circulating fluidized bed (CFB) combustion. This fly ash contains around $7-8$ wt% aluminum, of which 50% is assumed to be reactive. The ash contains alkalies and is mixed with process water of low pH containing industry acid. This produces an environmental gypsum which is used to rehabilitate the island and refill old limestone quarries. The intention is to rebuild the island to once again become an idyllic oasis for the general public [13].

NOAH discovered that the aluminum in the fly ash would react with water and produce hydrogen. This was discovered as the ash is mixed with process water for the production of the environmental gypsum. The possible

reactions between aluminum and water are presented in Chapter 2. At the moment, the hydrogen is not utilized or collected. NOAH's intention is to find a potential application for the produced hydrogen, and not letting this valuable by-product go to waste. The hydrogen could be used for several applications which can save costs and decrease the need for energy supply from external sources.

The hydrogen could be used for power production with the application of fuel cells, or as a diesel replacement. Hydrogen has the possibility to be used as a fuel for heavy machinery at the plant, for large transportation vehicles, such as the ferry connecting the island to the main land, but also for smaller, personal vehicles. Another option is to combust the hydrogen gas directly and utilize the heat produced, for instance in steam production.

In addition to the economical aspect, making the company greener is important. Utilization of an available by-product in place of fossil fuels, energy from non-renewable resources or to reduce transport is beneficial for both the company and the planet.

The possibility of selling the hydrogen has been investigated by NOAH, but the produced quantity has proved to small for this purpose. Thus, NOAH is primarily looking into on-site applications for the hydrogen. The alternatives for utilization of the gas will be further discussed in Chapter 3 and 4.

The specialization project involved a preliminary techno-economic assessment using data from NOAH's plant for hazardous waste at Langøya. The preliminary study describes a system for production and storage of hydrogen for further usage. This included a reactor for the aluminum-water reaction, a compression train and a storage tank. These three steps are the base case for the project and will be further described in Chapter 3. For the base case, the hydrogen was compressed to 350 bar, with the purpose being for usage in power production or as heavy vehicle fuel.

The production of hydrogen was assumed to be 180 tons per year and 50 kg/h, and the hydrogen content was discovered to be high enough for use in fuel cells. Furthermore, it was discovered that the gas requires purification for removal of impurities. The real composition of the gas was at this stage unknown.

The previous work estimated a total cost for the project at 2.79 MUSD without installation and 7.95 MUSD with installation, but there were a lot of uncertainties related to the estimation of these costs. The compressors and the reactor were found to be the main contributors to the costs. Over a ten

year horizon, the hydrogen production cost was found to be 4.4 USD/kgH_2. Open literature presented comparable production costs, and showed that the production was competitive with several other production methods from renewable sources.

1.2 Objective and outline

The objective of this thesis is to build upon what was discovered in the previous work. This will include a new investigation of the previous work with updated gas composition, and two application alternatives for the hydrogen. During the time of the thesis, NOAH performed an analysis of the composition of the produced hydrogen gas. This gave the opportunity to look into the required purification for reaching a composition applicable for usage in fuel cells. Purification and usage in fuel cells is one of the investigated alternatives, while the other is process heat production by direct combustion of the gas stream. The goal of the project is to investigate the implementation and feasibility of these alternatives, and to look into if they could be used to replace parts of current energy sources or process utilities.

The thesis will first present relevant background for work in the project. This will include technologies for utilization, hydrogen quality specifications and possible purification technologies. The base case and the two alternatives will be described in detail in Chapter 3. This chapter will present how the work in this project was performed and will describe the simulation setups of the alternatives. The chapter will also present the methods for sizing and estimation of the cost of the equipment in the project, in addition to assumptions and parameters of the alternatives. The results of the thesis will then be presented and discussed. This will include a discussion on the purification method found most suitable for fuel cell application, as well as the results and discussion of the two alternatives, and how the results compares to the open literature and NOAH's needs. Afterwards, the practical and economic feasibility of the alternatives will be compared and discussed. The conclusion and future work will be presented in the end.

Chapter 2

Background

This chapter will present relevant background for the thesis which will be used and referenced in the following chapters.

2.1 Water-aluminum reaction

The most stable reaction that takes place between aluminum and water at ambient temperature and up to 280 °C is shown in Equation 2.1.1 [14] The reactions shown in Equation 2.1.2 and 2.1.3 does also occur, but are less stable for the temperature interval.

$$2\,\mathrm{Al} + 6\,\mathrm{H_2O} = 2\,\mathrm{Al(OH)_3} + 3\,\mathrm{H_2} \tag{2.1.1}$$

$$2\,\mathrm{Al} + 4\,\mathrm{H_2O} = 2\,\mathrm{AlO(OH)} + 3\,\mathrm{H_2} \tag{2.1.2}$$

$$2\,\mathrm{Al} + 3\,\mathrm{H_2O} = \mathrm{Al_2O_3} + 3\,\mathrm{H_2} \tag{2.1.3}$$

The thermodynamics of the reaction is shown in Table 2.1. The table shows the enthalpy ΔH, entropy ΔS and Gibbs free energy ΔG for the reaction in Equation 2.1.1. This data show that the reaction is spontaneous for the conditions of this project, as the Gibbs free energy is negative for the interval.

2.2 Fuel cells

Fuel cells produce electricity and heat by utilizing the electrochemical reaction between hydrogen and oxygen as fuel, forming water. There exist

Table 2.1: Thermodynamics of the reaction shown in Equation 2.1.1 [14].

T [°C]	ΔH [kJ/mol H_2]	ΔS [J/K]	ΔG [kJ/mol H_2]
0	−277	26.2	−284
100	−284	3.29	−285

lots of different types of fuel cells, but the main principle remains the same. The basic principle of the fuel cells is to utilize the two electrochemical half reactions of the oxidation reaction. These reactions happens separately at the anode, Equation 2.2.1 and the cathode, Equation 2.2.2 [15].

$$H_2 \rightleftharpoons 2\,H^+ + 2\,e^- \tag{2.2.1}$$

$$\frac{1}{2}\,O_2\,2\,H^+ + 2\,e^- \rightleftharpoons H_2O \tag{2.2.2}$$

The separation of these reactions forces the generated electrons to flow through an external circuit, creating an electric current which can be utilized to produce energy. The separation is made using of an electrolyte which is a material that allows ions, but not electrons, to flow through. The main difference between the different type of fuel cells are what kind of electrolyte they employ [16].

The main types of fuel cells for hydrogen usage are phosphoric acid fuel cells (PAFC), molten carbonate fuel cells (MCFC), solid oxide fuel cells (SOFC), alkaline fuel cells (AFC) and proton-exchange membrane, or polymer electrolyte membrane, fuel cells (PEMFC). PEMFCs and SOFCs are of most interest for this thesis and will be looked at in more detail.

PEMFCs operates at 80 °C, while SOFCs operates in the range of 600 − 1000°C. PEMFC employs a polymer membrane as the electrolyte, while SOFC use a ceramic membrane. PEM fuel cells are the most utilized as they have a high power density, low temperature, and compact size. The downside is that they require high purity hydrogen [9]. SOFCs have a high efficiency and are flexible when it comes to the fuel [15].

PEMFCs are the best suited for use in vehicles as they have high density, quick start up, low weight and low operating temperature. SOFCs are more suitable to stationary applications due the temperature requirement. For

this purpose they can be more applicable than PEMFCs due to their high efficiency, high power output due to the high operating temperature and fuel flexibility.

If the fuel is not of sufficient quality, impurities can cause severe and irreversible damage to the fuel cell which negatively affects the performance and/or the life time of the fuel cell [1]. The impacts of some common impurities will be presented.

Water may reduce the membrane proton conductivity and cause corrosion of metal components of the cell. **Inert gas** can diffuse into the hydrogen and cause dilution, which would decrease the electric potential. **Carbon dioxide** will have a dilution effect on the hydrogen. High concentrations may lead to conversion into carbon monoxide through the revers water-gas shift reaction, which then leads to catalyst poisoning. **Carbon monoxide** will as mentioned lead to catalyst poisoning by binding to the active sites of the catalyst. **Sulfides** will adsorb on the active catalyst sites and will then react with the catalyst to form stable sulfides, which leads to irreversibly damage to the catalyst and the fuel cell. **Ammonia** can reduce proton conductivity and may also block the active sites of the catalyst through adsorption on the surface of the catalyst. **Particulate matter** will adsorb on the catalyst, can block the filter and damage and/or destroy components of the fuel cell [9].

2.3 ISO 14687

ISO 14687 [17] is an ISO standard which specifies the required hydrogen fuel quality for proton-exchange membrane (PEM) fuel cells. The standard should be followed to ensure the expected quality, safety and efficiency of the product. PEM fuel cells is the most applicable type of fuel cell for the purpose in this project and for usage in vehicles [18]. The standard provides concentration limits for several types of fuel cell applications. Table 2.2 shows the limits for the most relevant constituents of the gas. The values are specified for PEM fuel cell road vehicle applications.

2.4 Gas composition analysis

The composition of the produced gas was analysed by NOAH together with SINTEF early 2022. The exact results and composition will not be presented here as they are confidential and for internal use in the company at this point

Table 2.2: Limits for the most relevant components as of *ISO 14687*[17]. The values are specified for PEM fuel cell road vehicle applications. Phosphine (PH_3) and nitrous oxide (N_2O) do not have a specified limit in the standard. The values are based on mole.

Component	ISO 14687 limit
H_2	min 99.97%
H_2O	5000 ppb
CO	200 ppb
CO_2	2000 ppb
COS	4 ppb
CH_4	100000 ppb
NH_3	100 ppb
PH_3	-
N_2O	-

in time. The composition used for the simulations in this project is based on the composition from this test performed by SINTEF and NOAH.

The results showed that the hydrogen gas contains around 200000 ppb (parts per billion) of impurities. The content of the different impurities were compared with their limit from *ISO 14687* to decide the required amount of cleaning. Ammonia (NH_3) is reported as one of the largest and most problematic impurities, while methane (CH_4), nitrous oxide (N_2O), carbonyl sulfide (COS) and carbon monoxide (CO) also are significant impurities. A significant amount of water is also present in the gas and will have to be removed.

It is important to mention, as SINTEF also states, that the ISO standard is not an absolute limit for the impurity content a fuel cell can handle. However, the composition test confirmed the assumption that the gas needs purification to be applicable for PEM fuel cells.

2.5 Hydrogen purification

High hydrogen purity is crucial to ensure that hydrogen fuel cells run properly. Hydrogen purification is therefore important for providing this high quality. Purification is needed for most commercial production methods of crude hydrogen. This includes coal gasification, natural gas reforming, by-product hydrogen and electrolysis of water. Lots of hydrogen purification

technologies exist and they can be classified generally as either physical or chemical methods. Physical methods include adsorption, low-temperature separation and membrane methods. Chemical methods include metal hydride separation and catalysis methods. The selection of purification methods is dependent on production source of the hydrogen and the application [9].

Pressure swing adsorption is the most applied technology, but is generally more suited for production at medium or large scale. For small scale production, < 1000 Nm^3/h, PSA is not very suitable due to requiring much space, including low flexibility and adaptability. Low-temperature separation, metal hydrides or Pd-membranes are more applicable at this scale. New membrane technology currently in the research and development stage are expected to be the best option in the future. However, it should be noted that the existing hydrogen purification methods are limited, and still have difficulties with reaching the required standard for fuel cells. It is advised to adopt at least two technologies for reaching the required purity [9].

The following sections will present more details on some investigated hydrogen purification methods. Wet scrubbing will be described in more detail as it is used further in the project. It is a simple method that is easy to implement. PSA and membranes are two of the most common methods for reaching high purity levels [1]. These will also be described in more detail. A few other cleaning methods which were looked at will be summarized.

It should be noted that most purification and cleaning methods found in the open literature handles gas streams with different composition than the one in question in this project. The main difference is the already high hydrogen fraction observed. The impurities are though similar, but of lower order of magnitude than most compositions studied in the literature.

2.5.1 Wet scrubbing

Scrubbing is a type of process for removal of pollutants and impurities in a gas stream. In a wet scrubber, a scrubbing liquid is used for the removal of the pollutants, which can be both particulate matter and gaseous. The removal happens through counter-current washing with the liquid. The scrubbing liquid can for instance be water, an aqueous solution with sodium hydroxide, NaOH, or an amine solution.

For scrubbing, it is important to ensure good contact between the gas and liquid. For scrubbing of gaseous pollutants, which is classified as absorption,

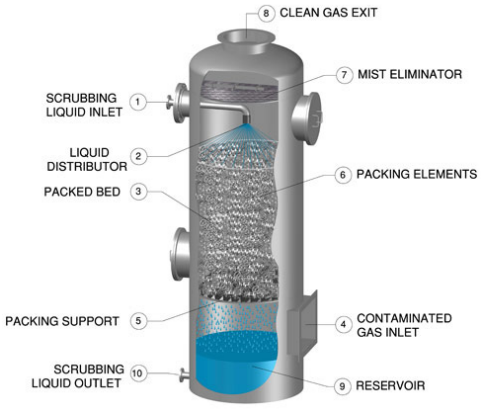

Figure 2.1: Illustration of a common wet scrubber using packed bed [19].

packing is commonly used to enhance the contact area. The gas is fed at the bottom of the scrubber vessel and then passes through the packed bed where the contact with the scrubbing liquid occur. Impurities are collected in the droplets which then is collected in the demister, or absorbed into the liquid. Figure 2.1 shows an illustration of a common wet, packed bed scrubber.

Wet scrubbing is a simple process that requires small space, have a low capital cost, high flexibility [20], while also promoting easy regeneration and reusability of the scrubbing liquid [21].

Scrubbing with amines is another common scrubber configuration. However, this is related to higher complexity due to amine poisoning, treatment of the amines and recovering gas, and disposal of the amines.

2.5.2 Pressure swing adsorption (PSA)

Pressure swing adsorption is a well-studied method for removing impurities and purifying gas streams. It is a universal method which is effective for removal of most contaminants [9]. PSA is the most applied method for hydrogen purification. Hydrogen is well suited for purification using PSA due to it being significantly different when it comes to static capacity, than most other gas molecules, and is then adsorbed to a much lower degree than others [22] [23].

The basic principle of pressure swing adsorption is using solid sorbents to adsorb impurities at high pressures (adsorption step) and subsequently desorb them at lower partial pressures (regeneration step). The purified gas

stream will exit the PSA at a pressure level close to the inlet [23].

The process is cyclic and usually utilizes at least to adsorption vessels. This means that when the adsorbent in one vessel has reached its capacity, the gas stream can be redirected to the other vessel, while the first goes through its regeneration step. Figure 2.2 shows a flow scheme of a common PSA configuration.

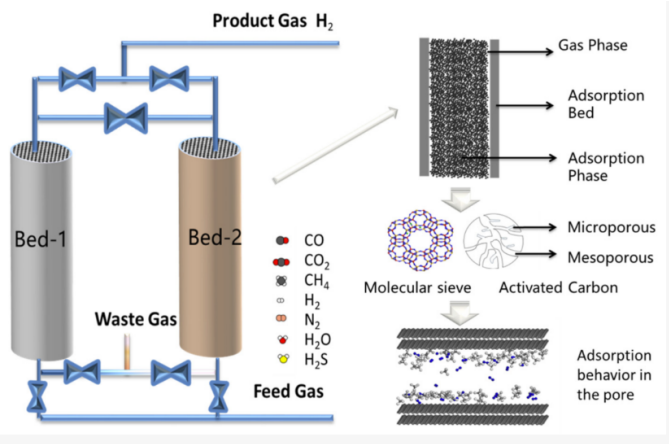

Figure 2.2: Flow scheme for a common PSA process [9].

Common adsorbents are zeolite molecular sieves, activated carbon or alumina and silica gel. For purification of hydrogen, two-layered bed adsorption columns using both activated carbon and zeolites is usually used for ensuring sufficient removal of different impurity types. Literature generally reports hydrogen purity levels from $98-99.999\%$ for PSA and recovery from $70-90\%$ depending on the adsorbent, number of beds and configuration [24] [9] [23] [5].

This type of process is complex and energy intensive, and it also can be impractical and not economically viable for lower flow rates.

2.5.3 Membranes

Purification through membranes can be a very effective technology when utilizing highly selective membranes. The basic principle behind membrane separation is that the membrane, a thin layer of a material, only allows specific kinds of species to pass through by permeation. The material which flows through the membrane is called the permeate. The material that does not pass through the membrane is called the retentate. The speed of

which species pass through the membrane is varying, and the ones flowing fast through the membranes can accumulate in the permeate. This makes it possible to separate components of a gas mixture from the others [25]. Figure 2.3 illustrates the principle of membrane separation of hydrogen.

Different types of membranes have varying selectivity for different species. A high selectivity for a component means that the membrane is good for purification of this component and can achieve a high purity of the component in the permeate. The driving forces of membranes are the difference in pressure, concentration and potential. Normally used membrane materials are metal and polymer membranes, but nanomaterials and metal-organic frameworks (MOFs) are also used. The most used metal membrane types are the palladium (Pd) membranes, which have very high hydrogen permeability. However, they are susceptible to hydrogen embrittlement at low temperature, but this can be solved with alloys. They are also related to high manufacturing cost [9].

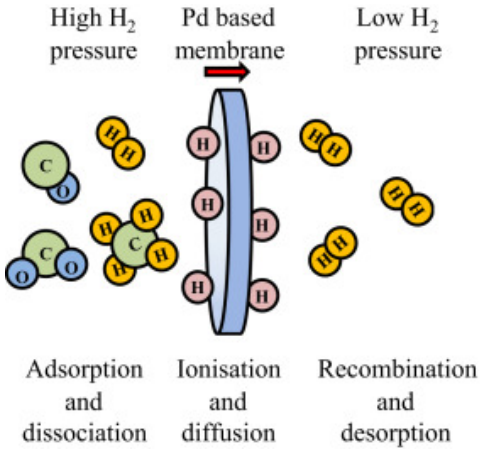

Figure 2.3: Simple illustration of the principle of membrane permeation [26].

Membrane separation has advantages of being flexible and a relatively simple operation. They have a compact structure, low energy usage and are environmentally friendly. The efficiency of the membranes is very dependent on the development of membranes with a very high selectivity for hydrogen.

2.5.4 Others

Cryogenic distillation is a common method used for hydrogen purification. It is however a complex and very energy intensive process. **Metha-**

nation was investigated, but not used due to low amounts of methane, not promoting removal of other impurities and that methanation rarely achieve a purity higher than 98%.[27]. **Catalytic hydrolysis of carbonyl sulfide** was studied for removal of COS, but it is not reported to reduce the impurity to the fuel cell standard. It also produced hydrogen sulfide, which is problematic. **Thermal or catalytic conversion** using the water-gas shift reaction for production of more hydrogen using carbon monoxide was also looked into. There is an abundance of water in the stream, but only trace amounts of carbon monoxide, which would lead to ineffective removal. A combination of **potassium hydroxide and methanol** was also studied. It is effective for COS removal, but is better suited for removal of impurities in liquid streams. **Hydrodesulfurization** is another method for removal of sulfur, but the process uses hydrogen for the removal. It is therefore not an alternative for this purpose.

2.6 Fired heaters and combustion

Fired heaters area heat exchangers that are heated by the products of combustion of a fuel. These are used when high temperatures and flow rates are needed, and include furnaces and boilers. For lower duties up to 45 MW, it is common to use small vertical cylindrical fired heaters, while cabin furnaces of larger size are used for higher duties[25].

Steam boilers are a type of fired heater where steam is produced. They contain a combustion chamber where the fuel and air are combusted. The boiler can, among other setups, contain a water container or tubes with passing water. The water in the tubes is heated and evaporated for producing high pressure steam. A simple illustration of steam production in a boiler using water tubes is shown in Figure 2.4.

Emissions from fired heaters are significant contributors to atmospheric emissions. Thus, they have to be regulated. Some general emission problems of fired heaters are introduced.

Carbon monoxide CO, unburned hydrocarbons and soot can be formed by incomplete combustion. This problem can be minimized by using at least 20% excess air in the combustion. Sulphur oxides can be formed by combustion of fuels containing sulphur or metals, and is mainly a problem for combustion of heavy fuel oils. Formations of nitrogen oxides, NOx, is another problematic emission type that occurs with combustion using fired heaters. This emission is usually worsened by utilization of excess air. The

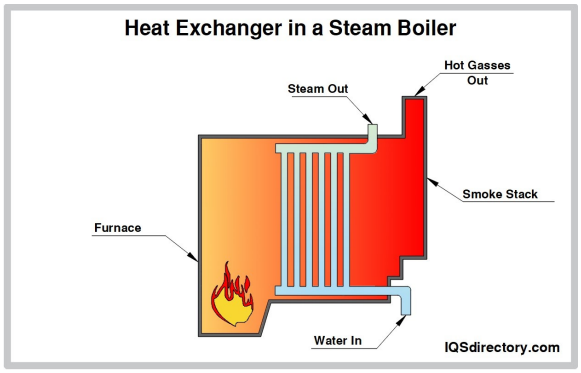

Figure 2.4: Simple illustration of steam production in a boiler [28].

formation is instead generally controlled by special burner designs, or by steam injection or flue gas recirculation to reduce the flame temperature. Carbon dioxide CO_2 will form when combusting hydrocarbon fuels. It can be recovered with for example scrubbing of the flue gas [25].

Chapter 3

Methods

This chapter will present the methods that are used to simulate and investigate the cases of this project. It will present the main parameters, assumptions and necessary information for understanding the following results and discussion.

3.1 Base case

This work of the thesis is, as mentioned earlier, a continuation of earlier work[12], and the base case is consequently kept.

The original base case describes the hydrogen production from the reactor to storage. The process was divided into three stages: the main reactor, the compression train and the storage tank. Figure 3.1 presents a simplified flow sheet of the three stages of the base case. The compression train is presented in the brackets. The train consists of five compression cycles. As each cycle consists of a heat exchanger, a separator and a compressor, illustrated with subscript i. An additional heat exchanger (HX106) and separator (S106) is added after the compression train before storage.

In the previous work, the reactor and the storage tank were modeled in Microsoft Excel, while the compression train was simulated in Aspen Plus V10. The simulation flow sheet from Aspen Plus for the base case is shown in Appendix E.

The operating parameters for the reactor of the base case are shown in Table 3.1. The flow rate is given for the outflow of the reactor.

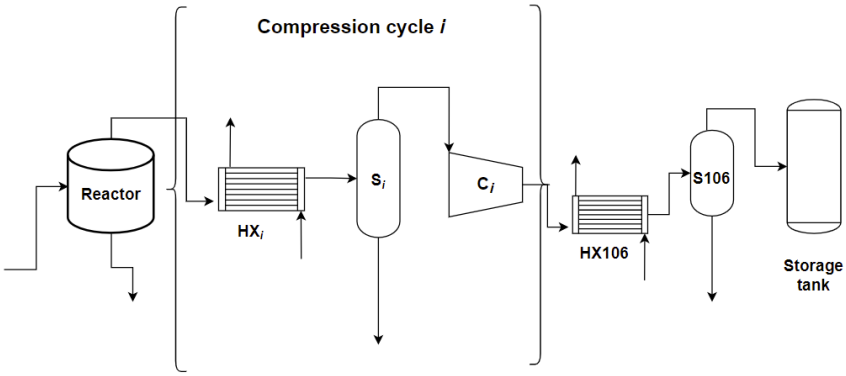

Figure 3.1: Simplified flow sheet of the base case. The compression train is illustrated with the brackets. It consists of five compression cycles.

The model assumed a hydrogen production of 50 kg/h. This production was estimated from data from NOAH, with an assumed hydrogen production of 40 mL/g ash. NOAH receives up towards 50000 tons of fly ash each year. They use an ash/water ratio of around 1.4 for the gypsum production, which then requires around 70000 tons of water per year. For this analysis, 250 operating days per year and 14 operating hours per day were assumed. This gives 3500 operating hours per year. A residence time of three hours was assumed. The mass density for hydrogen is 0.0898 g/L [29] at standard temperature and pressure. With these assumptions, the yearly hydrogen production is 180 tons per year. Divided by the number of operating hours each year gives the assumed hydrogen production of 50 kg/h. The impurities are included in mass flow, while the remaining flow consists of water. The water content was estimated as described in Appendix B.1.

Table 3.1: Operating parameters for the reactor of the base case. The flow rate is given for the gas outflow from the reactor.

Parameter	Value
Flow rate	27.87 kmol/h
	106.00 kg/h
Temperature	50 °C
Pressure	1.1 bar
H_2 production	40 mL/g ash
Residence time	3 h

As the gas composition analysis was performed during the stage of the Master's thesis, the main gas stream composition from the original base case contained only hydrogen, water and an assumed 200 ppm of ammonia. For the present work, the base case was therefore updated with the new composition after the analysis was performed. The new composition is given in Table 3.2. This composition is used for the hydrogen gas stream for all following simulations.

Table 3.2: Composition of the reactor outflow. This is the composition which is used for all simulations in this thesis. The flow, temperature and pressure of the stream are given in Table 3.1.

Component	Mole fraction
H_2	0.8883
H_2O	0.1115
NH_3	9.2E-05
CO	1.8E-06
CO_2	1.2E-06
COS	4.1E-08
CH_4	6.8E-05
PH_3	5.3E-07
N_2O	8.8E-06

The compression train was simulated in Aspen Plus V10 using the Peng-Robinson thermodynamic package. In this process the hydrogen gas stream was compressed from 1 bar to 350 bar. This pressure is suitable for storage and for the use in heavy vehicles. The compression train consists of five compression cycles. Each cycle has three steps: compression, intercooling and a separator for removal of formed condensate.

Through intercooling, the gas temperature at the inlet of each compression cycle was kept at 20 °C. This is important for achieving efficient compression. The cooling water flow rate used was 1400 kg/h at 10 °C for each intercooling stage. The outlet temperature of the cooling water was approximately 30 °C, for safe disposal. The pressure of the cooling water was specified to be roughly the same as the gas at the hot inlet, to avoid high pressure differences which can lead to operating problems.

Flash separators were used to remove the condensed liquid after the intercooling. The separators were using an operating temperature of 20 °C with no pressure drop. The compressors were using a compression ratio of 3.17

and were set up as isentropic.

The storage tank was modeled in Excel. The storage tank was designed for storing one day of production of hydrogen, 700 kg, at 350 bar and 20 °C.

3.2 Application alternatives

This section will describe the two alternatives for the utilization of the hydrogen, which are investigated in this thesis.

3.2.1 Alternative 1: Fuel cells

The first alternative is a direct continuation of the base case. The aim of this alternative is to implement one of the cleaning methods discussed in the following section, to achieve a high purity hydrogen gas stream ready for storage. The goal is to clean the gas to achieve the required level of purity below the limits of the discussed ISO standard. This is necessary for the possibility of using the hydrogen in PEM fuel cells, which then could be used to produce electricity or power vehicles. The implementation and choice of cleaning method is therefore the most important part of this alternative.

In this project, the alternative is implemented with a water scrubber operating at 35 bar. Several other scrubber configurations were also investigated. All configurations will be discussed in more detail in the description of the simulations of the scrubbers and in the results, where they will be compared. The reactor and storage tank of the base case remain the same. The scrubber is implemented as the step before the fourth compressor which takes the gas stream from 35 bar to 111 bar. The simplified flow sheet of Alternative 1 is shown in Figure 3.2.

3.2.2 Alternative 2: Process heat production

The second alternative that was investigated was to combust the produced hydrogen gas directly for heat production. The heat could then be utilized on-site. In this project, a boiler was used to produce the steam. The hydrogen gas stream was fed to the boiler with 20% excess air to produce heat for the boiling and flue gas at 120 °C. The goal was to produce steam at 185 °C and 11 bar which was of use for NOAH, and quantify how much of their need that could be covered. The steam would be used for heating and evaporation of brine, in another project NOAH is working on, *Resalt* [30],

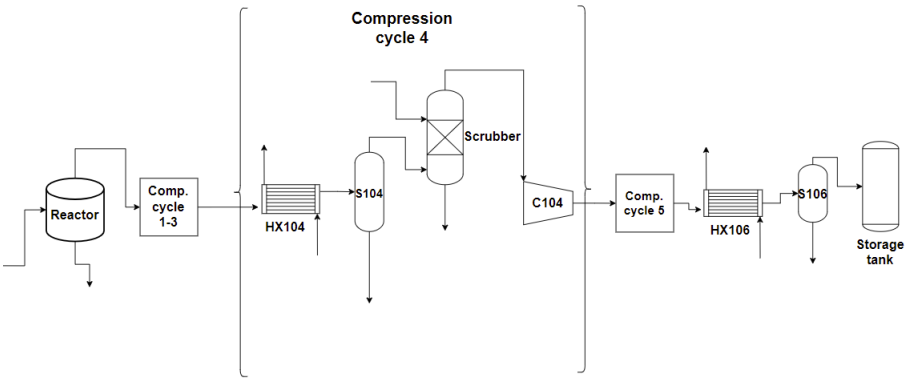

Figure 3.2: Simplified flow sheet of Alternative 1. The compression cycle where the scrubber is implemented is shown in the brackets. Compression cycle 1 to 3 and 5 are illustrated by the squares. They are equal to the cycles shown in Figure 3.1.

which focus on salt recovery. The steam would be part of a loop and would be recycled back to the proposed process.

This alternative would avoid the need for purification, compression and storage of the gas, which makes the project less complex and less expensive. The reactor is still included for the production of the hydrogen gas.

Figure 3.3 presents a simplified flow sheet of Alternative 2. The steam is produced in the boiler and is utilized for the brine evaporation. The low pressure (LP) liquid is then pumped to high pressure (HP) liquid before it re-enters the boiler.

3.3 Cleaning methods

Chapter 2 presented the conventional cleaning methods for removal of the most important impurities in the hydrogen gas stream. Most of them could be utilized in this scenario for reducing the concentration of the impurities to levels accepted for fuel cell usage.

For the work in this project, wet scrubbing with water and sodium hydroxide were selected as the methods of investigation. They were selected based on the complexity of the process, the impurities removed, and expected cost. Implementation of the methods in the simulation tool was also taken

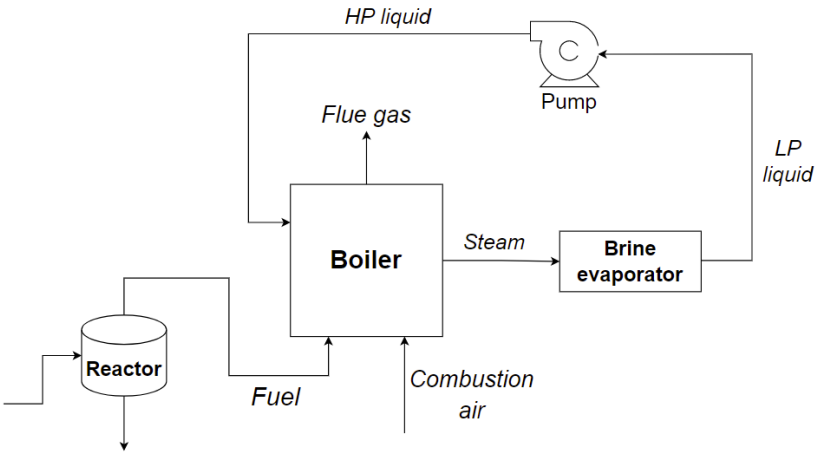

Figure 3.3: Simplified flow sheet of Alternative 2. LP and HP indicates low and high pressure.

into account for the consideration. The application of other conventional technologies mentioned in this work, especially PSA and membranes, will be a part of future work.

3.4 Simulation description

This section will describe the simulation setup for the two alternatives described earlier. A new simulation, with the updated composition in Table 3.2, was performed for the base case. Aspen Plus V10 was used for the simulations. The simulation flow sheets from Aspen Plus for the models are shown in Appendix E.

3.4.1 Alternative 1: Fuel cells

Compression model with scrubber

For this alternative, seven cases with varying scrubber configurations were simulated. This was done to find the best scrubber option to use. This was then implemented in the compression model from the base case. The flow and composition of the gas streams were extracted from the base case simulation. The stream data for the inlet and outlet for the scrubbers are shown in Appendix A.1.

Five scrubber cases (A-E) were originally investigated. The cases were based on the different pressures from the compression train and the two absorbents available. The first, Case A, was a scrubber using pure water as the scrubber liquid and a L/G ratio of 2.1. The operating pressure was 1.1 bar, which is the pressure of the reactor outflow of the base case. It was expected that the effectiveness of the cleaning would increase if the operating pressure was increased. Two additional water scrubbers (Case B and C) at 11 bar and 35 bar were therefore investigated. The operating pressures come from the pressure of the hydrogen gas stream after two and three compressions in the base case, respectively. Two scrubbers using 10 wt% of sodium hydroxide as the liquid absorbent (Case D and E) at operating pressures of 11 bar and 35 bar were also investigated. Two additional scrubber cases, Case X and Case Y, were also investigated. They are based on Case A and Case C respectively with increased liquid-gas ratios. This increases the contact area between the liquid and the gas, and should result in better cleaning. The scrubber configuration for each case is summarized in Table 3.3.

Table 3.3: Overview of the different scrubbers that were investigated in Aspen Plus. The fraction of H_2O and NaOH are based on mass.

	Pressure [bar]	H_2O frac.	NaOH frac.	L/G
Case A	1.1	1	0	2.1
Case B	11	1	0	2.1
Case C	35	1	0	2.1
Case D	11	0.9	0.1	2.1
Case E	35	0.9	0.1	2.1
Case X	1.1	1	0	10.4
Case Y	35	1	0	3.5

The scrubbers were simulated in Aspen Plus by using a RadFrac absorption column without a condenser or a reboiler. They were set up using equilibrium calculations and with 10 stages. Ceramic Berl saddles with a diameter of 13 mm were chosen for the packing. The choice was based on specifications for this type of case in Sinnott and Towler (2020) [25]. The dimension was specified to have a ratio of tower diameter/packing diameter towards 15/1. A ratio higher than this is suggested as a rule of thumb [31]. The liquid holdup was specified as 0.001 m^3. The section packing was set to be 0.5 m. The diameter of the column was calculated as shown in Appendix D.1. Table 3.4 summarizes the parameters and specifications for the columns.

Table 3.4: Specifications for the RadFrac column used to simulate the scrubber in Aspen Plus. These specifications apply for all scrubber simulations.

Parameter	Setting
Calculation type	Equilibrium
Stages	10
Packing	Berl saddles
Packing dimension	13 mm
Section packing height	0.5 m
Liquid holdup	0.001 m^3

Equation set 3.4.1 shows the reactions used for the water scrubber in the simulation. The reactions were proposed by the Aspen Plus V10 databank.

$$\begin{aligned}
NH_3 + HCO_3^- &\rightleftharpoons H_2O + NH_2COO^- \\
NH_3 + H_2O &\rightleftharpoons OH^- + NH_4^+ \\
H_2O + HCO_3^- &\rightleftharpoons CO_3^{2-} + H_3O^+ \\
2\,H_2O + CO_2 &\rightleftharpoons HCO_3^- + H_3O^+ \\
H_2O + HS^- &\rightleftharpoons H_3O^+ + S^{2-} \\
H_2O + H_2S &\rightleftharpoons H_3O^+ + HS^- \\
2\,H_2O &\rightleftharpoons OH^- + H_3O^+
\end{aligned} \tag{3.4.1}$$

Equation set 3.4.2 shows the reactions used for the NaOH scrubber in the simulation. The reactions were proposed by the Aspen Plus V10 databank.

$$\begin{aligned}
NH_3 + HCO_3^- &\rightleftharpoons H_2O + NH_2COO^- \\
NH_3 + H_2O &\rightleftharpoons OH^- + NH_4^+ \\
H_2O + HCO_3^- &\rightleftharpoons CO_3^{2-} + H_3O^+ \\
2\,H_2O + CO_2 &\rightleftharpoons HCO_3^- + H_3O^+ \\
H_2O + HS^- &\rightleftharpoons H_3O^+ + S^{2-} \\
H_2O + H_2S &\rightleftharpoons H_3O^+ + HS^- \\
2\,H_2O &\rightleftharpoons OH^- + H_3O^+ \\
NaOH &\longrightarrow OH^- + Na^+
\end{aligned} \tag{3.4.2}$$

Scrubbing with water at 35 bar was found to be the best choice. This is discussed more in Chapter 4. The scrubber was implemented in the simulation between the third (C103) and the fourth (C104) compressor, after intercooling and the separator. This is illustrated in Figure 3.2. The same configuration and reactions as in the scrubber simulations were used. They are given in Table 3.4 and in reaction set 3.4.1.

3.4.2 Alternative 2: Process heat production

Before simulating the process heat production in Aspen Plus, the necessary amount of combustion air was calculated. The air composition was calculated with an assumed 20% excess air to ensure complete combustion, and assuming 80% air saturation. The calculation is shown in Appendix C.1.

Alternative 2 of the applications was simulated in Aspen Plus V10 using the Peng-Robinson thermodynamic package. The boiler and combustion were simulated using a stoichiometric reactor based on fractional conversion. The reaction specified was

$$2\,H_2 + O_2 \longrightarrow 2\,H_2O \tag{3.4.3}$$

and the global conversion of H_2 of 1 was specified. This means that the reactor was based on 100% conversion of the hydrogen gas entering the reactor. The reactor outlet, flue gas, pressure and temperature were specified to 1 bar and 120 °C respectively. For producing the highest amount of steam, the flue gas temperature should be as low as possible, i.e. as much heat as possible is transferred. To ensure safe release of the flue gas, according to emission standards, the flue gas temperature must be at least 100 °C. 120 °C was chosen to ensure a good margin to the requirement.

For this type of reactor Aspen Plus can generate combustion reactions in addition to the reaction(s) specified. This was included in the simulation in this project. When applying this setting a NOx combustion product must be specified. Nitric oxide, NO, is the default and was chosen for this simulation.

The fuel gas entering the combustion reactor has a composition extracted from the base case. The fuel enters the reactor at 53 °C and 1.1 bar with a flow of 28.2 kmol/h. It contains 88.8 mole% hydrogen and 11.2 mole% water. The full composition is shown in Table 3.2.

The composition of the air required for combustion of the flue gas was calculated as described earlier. The mole flows are shown in Table 3.5. The air

flow enters at 25 °C and 1.1 bar with a flow of 78 kmol/h.

Table 3.5: Mole flows of the wet air for the combustion, with 20% excess air and 80% saturation.

Component	Mole flow
Oxygen	15.0 kmol/h
Nitrogen	55.7 kmol/h
Water	6.9 kmol/h

The steam loop was simulated in a separate loop in the simulation. An energy stream from the boiler to a heater in the steam loop was therefore set up. The energy stream, with the heat produced in the combustion, was used as the input of the heater. This heater produced the steam in the steam loop. The target for the steam production was steam at 185 °C and 11 bar. The mass inflow of water to the heater was adjusted to reach the targets for temperature and pressure, while keeping the vapor fraction as close to 1 as possible. This resulted in using a water inflow of 2072 kg/h. The heater was set up with zero pressure drop.

The utilization of the produced steam was then simulated by heat exchanging with 12 610 kg/h (700 kmol/h) of water at 20 °C and 11 bar. The pressure was set to be equal to the steam. After the heat exchanger the steam was specified to be at 50 °C and 0.2 bar, producing low pressure liquid water. The heat exchanger has a pressure drop of 10.8 bar for the hot stream. The values for temperature and pressure were chosen together with NOAH. The heat exchanger was set up as counter-current with a minimum temperature approach of 5 °C.

The liquid was then fed into a pump which pressurizes the stream from 0.2 bar to 11 bar, producing high pressure liquid water. The liquid stream then re-enters the heater, which simulates the boiler, and is used to produce steam at 185 °C and 11 bar. The efficiency of the pump was set to 29.6% by Aspen Plus. This concludes the steam producing loop for utilization of the heat produced by the combustion.

3.5 Sizing and cost estimation

This section will present how the sizing and cost estimation for the base case and the two alternatives were performed. Further details on the calculations will be shown in Appendix D.1 and D.2.

The sizing estimations were primarily performed using Aspen Plus V10 and methods described in *Chemical Engineering Design* by Sinnott and Towler[25]. The cost estimations for the equipment were mostly calculated using Equation 3.5.1, from Sinnott and Towler.

$$C_{pur} = a + b \cdot S^n \tag{3.5.1}$$

C_{pur} is the purchase cost of the equipment. a, b and n are cost parameters from Table 6.3 in Sinnott and Towler, which are specific the type of equipment. S is the size parameter for the equipment type.

The costs including installation were estimated using an installation, Hand factor, which is specific for the equipment type. Stainless steel 304 ss was used for all of the equipment that handle water. Other material selections will be specified. Cost escalation was accounted for using CEPCI[32], as Sinnott and Towler provides costs for Jan 2007. All costs were calculated both without and with installation included.

3.5.1 Base case

As described earlier, the base case is the same case that was studied in the specialization project. The only difference is the updated composition. The sizing and cost estimation will thus be the same. The change in composition did not cause any notable differences in the sizing and the following cost estimation. The sizing and cost estimation for the base case is therefore the same is in the earlier work[12].

The sizing parameter for the compressors of the compression train is the required power. This was obtained from the Aspen Plus simulation. The cost was calculated using Equation 3.5.1 with parameters for reciprocating compressors. The electricity cost for the compressors was also estimated using values from SSB[33] and DNB[34]. The required amount of kW h was based on the assumption of 250 operating days per year and 14 operating hours per day.

The sizing parameter for the heat exchangers is the required heat exchanging area. These were provided by the simulation in Aspen Plus. The cost was then calculated using Equation 3.5.1 for double pipe heat exchangers.

The sizing parameter for the separators is the shell mass. The design of the separators was first estimated using the method for vertical separators in

Sinnott and Towler using data from the Aspen Plus simulations. The shell mass was the estimated using the method given in the book, using a welded joint efficiency of 1 and a maximum allowable stress of $20ksi$ (1378 bar) for 38 °C under ASME BPV Code Sec. VIII D.1 from Table 13.2 in the book. The cost was then estimated using Equation 3.5.1 with parameters for a vertical pressure vessel in 304 ss.

The sizing parameter of the reactor is the volume and it was estimated in Excel using the assumptions stated earlier and the parameters in Table 3.1. The cost was estimated from Equation 3.5.1 for a jacketed, agitated reactor.

The sizing parameter for the storage tank is the shell mass. The tank was designed to be able to store one day of hydrogen production. The volume was then found using the density of the gas mixture at the storing conditions. This value was obtained from the simulation in Aspen Plus. The shell mass was calculated using the same method as with the separators. The cost was the estimated using Equation 3.5.1 for a vertical pressure vessel in 304 ss.

3.5.2 Alternative 1

As Alternative 1 is the combination of the base case and a scrubber, only the sizing and cost estimation will be presented in this section. The base case is presented earlier.

The sizing of the scrubber was performed in the Aspen Plus simulation using sizing calculations with Aspen Process Economic Analyzer (APEA). This provided an updated value for the diameter, as well as values for the packing height and the height of the vessel.

There were a lot of uncertainties related to the sizing using APEA. The parameters described in the simulation description, which are used as the starting point for the sizing with APEA, came with uncertainty. It was also unclear what some of the data from APEA actually described. The packing height given in APEA was one of these unclear values and seemed, based on experience, to be slightly low. The packing height was therefore scaled up by a factor of five. With the already high uncertainty, it was of interest to see if the scrubber cost, scaled up, would affect the total cost significantly. More details on the calculations and new assumptions are described in Appendix D.1.

The volume of the packing was then calculated based on the packing height and diameter of the vessel. The volume of the vessel was also calculated.

The shell mass of the vessel used for the cost estimation was calculated the same way as for the separators in the base case.

The sizing parameter for the packing is the packing volume. The sizing parameter of the vessel is the shell mass. The cost of the packing and vessel were estimated using Equation 3.5.1, using parameters for ceramic intalox saddles and vertical pressure vessels in 304 ss respectively. The cost of the scrubber is the sum of the packing and vessel cost. The total cost of Alternative 1 is the sum of the scrubber cost and the cost of the base case.

The cost of the fuel cells was not included in this estimation, but this will be discussed in Chapter 4.

3.5.3 Alternative 2

The cost estimation of Alternative 2 consist of the cost of the boiler and the pump used in the steam loop. The reactor cost from the base case is also included. The heat exchanger is not included as this would not be used in the real-life scenario. The heat exchanger is only included to illustrate the application of the steam and for creating a complete simulation of the steam loop.

The sizing parameter for the boiler is the produced heat duty, which is extracted from the simulation. The estimated cost of the boiler was then estimated using data for a cylindrical furnace and Equation 3.5.1. Data for a cylindrical furnace was used instead of data for boilers. The data for the boilers were meant for a much higher steam production and for a higher pressure than what was used in this project.

The sizing parameter for the pump is the volumetric flow in the pump. This data is extracted from the simulation. The cost was estimated using Equation 3.5.1 with data for a single stage centrifugal pump.

The cost of Alternative is then the sum of the boiler and pump cost.

Chapter 4

Results and discussion

This chapter will present and discuss the results of the project. The results from the simulations, including stream data, will be presented for the base case, Alternative 1: Fuel cells and Alternative 2: Process heat production. The cost estimation, including sizing, of all cases will be presented after. A further discussion on the feasibility of the alternatives will be presented in the end.

4.1 Simulation

4.1.1 Base case

Table 4.1 shows stream data for the inflow and outflow of the base case. The inflow is the flow exiting the reactor. The outflow is the compressed product stream which would be stored in the storage tank. The flow sheet of this case is shown in Figure 3.1.

Table 4.2 shows stream data for the flow that exits the named compressor. The total flow reduced as condensed liquid is removed in the separator. The mole fraction for all the streams is shown in Appendix A.2.1.

Table 4.3 shows the duties of all the compressors. The efficiency of the compressors were 72%. The power consumption of the compressors is small, but will give an increase in the cost.

Table 4.1: Stream data for inflow and outflow of the base case. The inflow is the outflow from the main reactor. The outflow is the product stream of the compressed hydrogen gas. The flows are given in kmol/h.

	Inflow	Outflow
Temperature [°C]	52.7	20
Pressure [bar]	1.1	352.1
H2	24.7595	24.7595
H2O	3.1085	0.0053
NH3	0.0026	0.0018
CO	5.0E-05	5.0E-05
CO2	3.2E-05	3.2E-05
COS	1.1E-06	1.1E-06
CH4	0.0019	0.0019
PH3	1.5E-05	1.5E-05
N2O	0.0002	0.0002
Total	27.87	24.77

4.1.2 Alternative 1

This section presents the results of Alternative 1: Fuel cells. The results from the simulations of the difference scrubber configurations will first be presented. The most effective configuration was implemented in the compression simulation which will be presented after.

Scrubber simulations

Table 4.4 shows the component removal as a percentage of the inlet flow of the component. As described earlier; Case A, B and C are water scrubbers at 1 bar, 11 bar and 35 bar, respectively. Case D and E are scrubbers with 10 wt% NaOH at 11 bar and 35 bar, respectively. The scrubbers operate with a liquid-gas ratio of 2.1. Additional stream data for the scrubbers are shown in Appendix A.1. The removal of water is negative due to the addition of some water to the gas stream during the scrubbing.

The effectiveness of the cleaning is best shown in Table 4.4, by comparing the component removal.

For scrubbing with water and NaOH at the same pressure, see Case C and Case E, it is clear that the water scrubber is more effective. It removes

Table 4.2: Stream data for the flows exiting the compressors in the base case. The flows are given in kmol/h.

	C101	C102	C103	C104	C105
Temp [°C]	179	179	179	180	182
p [bar]	3.5	11.1	35.0	111.1	352.1
H2	24.7595	24.7595	24.7595	24.7595	24.7595
H2O	0.4333	0.1358	0.0434	0.0144	0.0053
NH3	0.0022	0.0021	0.0020	0.0019	0.0018
CO	5.0E-05	5.0E-05	5.0E-05	5.0E-05	5.0E-05
CO2	3.2E-05	3.2E-05	3.2E-05	3.2E-05	3.2E-05
COS	1.1E-06	1.1E-06	1.1E-06	1.1E-06	1.1E-06
CH4	0.0019	0.0019	0.0019	0.0019	0.0019
PH3	1.5E-05	1.5E-05	1.5E-05	1.5E-05	1.5E-05
N2O	0.0002	0.0002	0.0002	0.0002	0.0002
Total	25.20	24.90	24.81	24.78	24.77

Table 4.3: Compressor duties for the compressor in the compression train of the base case. The efficiency of the compressors was 72%.

	C101	C102	C103	C104	C105
Duty	32.4 kW	32.1 kW	32.2 kW	32.8 kW	34.9 kW

significantly more of all components, although it adds more water to the stream. However, the water is not a problem as this will be removed with the following compression and flash separation. Increasing the operating pressure of the scrubber is also shown to be more effective. This is shown by comparing Case A to Case B and C, where significantly higher removal rates are shown for the higher operating pressures. Therefore, it is concluded that the water scrubber operating at 35 bar, Case C, is the most viable scrubber configuration at this liquid-gas ratio.

A higher liquid-gas ratio was tested for Case A and Case C, to see how it would affect the removal of impurities. The idea was that an increased ratio possibly could make Case A viable, which would simplify the process. This is the simplest configuration and water supply is not an issue at the plant. The liquid-gas ratio was increased up until 10.4 for Case A, which led to an increase in removal of impurities. Sufficient ammonia removal to fulfill the ISO standard was reached at a liquid-gas ratio close to 10. The removal of

Table 4.4: Component removal for the cleaned gas stream after the scrubbing. The component removal is given as a percentage of the component inlet flow.

	Case A	Case B	Case C	Case D	Case E
H2	5.6E-08	6.0E-07	1.8E-06	2.4E-07	7.4E-07
H2O	-17.86	-23.91	-25.72	-12.86	-14.05
CO	0.06	0.55	1.61	0.22	0.64
CO2	100	100	100	100	100
COS	2.96	26.66	76.61	10.58	31.18
NH3	47.55	100.00	100	62.02	99.91
CH4	0.46	4.30	12.44	1.71	4.96

COS also increased with increasing L/G, but was still not close to fulfilling the ISO standard.

For Case C the liquid-gas ratio was increased to 3.5 which led to sufficient removal of carbonyl sulfide to reach the requirement, in addition to complete removal of ammonia and carbon dioxide as in the lower L/G case. The remaining impurities were also further removed. Table 4.5 shows a comparison of the mole fractions of the cleaned gas stream for the water scrubber at 35 bar with liquid-gas ratios of 2.1 and 3.5.

Table 4.5: Comparison of the mole fractions of the outlet gas stream for the water scrubber at 35 bar at a L/G ratio of 2.1 (Case C) and 3.5 (Case Y).

Component	Case C	Case Y
H2	0.9992	0.9992
H2O	0.0007	0.0007
CO	1970 ppb	1950 ppb
CO2	≈0	≈0
COS	10.8 ppb	0.8 ppb
NH3	≈0	≈0
CH4	66500 ppb	60200 ppb

The results presented in the table show that the case with increased liquid-gas ratio, Case Y, is the best configuration for the scrubber. This scrubber configuration will therefore be used in the implementation of the scrubber in the compression simulation.

Additional stream data for the two water scrubbers with increased liquid-gas

ratios are shown in Appendix A.1.

Compression train with scrubber

Table 4.6 shows stream data for the inflow and the outflow of the compression train for the base case (without cleaning) and Alternative 1 (with cleaning). Scrubbing with water was used for the cleaning of the gas. The scrubber was implemented with an operating pressure of 35 bar.

Table 4.6: Overview of the inflow to the compression train, and the outflows for both the case with (w) and without (w/o) the scrubber. The flows are given in kmol/h.

	Inflow	Outflow (w/o)	Outflow (w)
Temperature	52.7 °C	20 °C	20 °C
Pressure	1.1 bar	352 bar	352 bar
H2	24.7595	24.7595	24.7595
H2O	3.1085	0.0053	0.0032
NH3	0.0026	0.0018	0
CO	5.0E-05	5.0E-05	4.8E-05
CO2	3.2E-05	3.2E-05	0
COS	1.1E-06	1.1E-06	2.0E-08
CH4	0.0019	0.0019	0.0015
PH3	1.5E-05	1.5E-05	0
N2O	0.0002	0.0002	0.0002
Total	27.87	24.77	24.76

Table 4.7 shows the mole fraction and material removal from the mentioned outflows.

Table 4.7 shows the effectiveness of the inclusion of the scrubber. The cleaned hydrogen gas stream has a hydrogen purity of 99.98% and fulfills the ISO standard, in contrast to the uncleaned stream. Ammonia, phosphine and carbon dioxide are removed completely, while carbonyl sulfide is removed to a sufficient level. Significant amounts of methane and nitrous oxide are removed, although the content of these never were an issue.

Even though 99.90% of the water content is removed, the mole fraction is still too high compared to the ISO standard. It contains 100 ppm of water, while the limit is 5 ppm. Additional removal of the water is still needed.

Table 4.7: Overview of the composition of the outflows and removal of impurities after the compression train with (w) and without (w/o) the scrubber. The composition is given as mole fractions. The material removal is given as a percentage of the inflow of the component to the compression train.

	Fraction (w/o)	Removed (w/o)	Fraction (w)	Removed (w)
H2	0.9996	3,7E-06	0.9998	3.2E-06
H2O	0.0002	99.83	0.0001	99.90
NH3	7.4E-05	28.45	0	100
CO	2.0E-06	1.7E-06	2.0E-06	2.73
CO2	1.3E-06	0.0003	0	100
COS	4.6E-08	0.0008	8.0E-10	98.26
CH4	7.6E-05	2.1E-05	6.0E-05	21.12
PH3	6.0E-07	0.0008	0	100
N2O	9.9E-06	0.0013	6.1E-06	38.70

Carbon monoxide is barely removed even with scrubbing. It is a stable molecule and will react very slowly with liquid water. Even though it is used for the water-gas shift reaction, which is favorable at lower temperatures, this involves water vapor. The reaction with liquid, as opposed to vapor, is significantly slower. Thus, no reaction between carbon monoxide and liquid water was proposed by the databank in Aspen Plus. The solubility of the gas at 25 °C is only 0.026 [35] g gas per kg water. Compared to for instance carbon dioxide at 1.5 [35] g gas per kg water, the solubility is very low. This leads to the component content to still be well above the limit of the ISO standard, and remaining a problem. Further removal is needed.

4.1.3 Alternative 2

Table 4.8 shows the heat production from the combustion. The value for MW h/year is based on 14 operating hours per day and 250 operating days per year.

Table 4.8: Heat production from the combustion of the hydrogen gas stream.

Heat production	1.54 MW	5400 MWh/year

According to Statistics Norway (SSB) the yearly total energy usage per household was 20 230 kW h in 2012 [36]. Data for later years were not available. This means that the energy production from the combustion of the

gas stream could cover the yearly energy usage of around 270 households. In real life this value may not be accurate due to heat loss and lower efficiencies, but it gives an idea of the scale and shows that the energy production is significant.

The pump which pressurizes the liquid stream from 0.2 bar to 11 bar has a duty and flow as shown in Table 4.9.

Table 4.9: Simulation data for the pump.

Data	Value
Flow	0.594 L/s
Duty	2.17 kW

Table 4.10 shows data and the composition of the hydrogen gas stream which fuels the combustion, the combustion air containing moisture and the flue gas exiting the combustion.

Table 4.10: Data and composition for the combustion fuel, wet air and flue gas. The flows are given in kmol/h.

	Fuel	Wet air	Flue gas
Temperature [°C]	52.7	25	120
Pressure [bar]	1.1	1	1
H2	24.9952	0	0
O2	0	15.12	2.6152
N2	0	56.88	56.88
H2O	3.15	7	35.1528
CO	5.0E-05	0	0
CO2	3.3E-05	0	0.0020
COS	1.2E-06	0	1.2E-06
CH4	0.0019	0	0
NH3	0.0026	0	0
NO	0	0	0.0031
NO2	0	0	0
PH3	1.5E-05	0	1.5E-05
N2O	0.0002	0	0
Total	28.15	79	94.65

Table 4.10 shows that all of the hydrogen, carbon monoxide, methane, am-

monia and nitrous oxide have been combusted. Mostly water, but also carbon dioxide and nitric oxide, have been formed. Nitrogen and carbonyl sulfide act as inerts. Some oxygen remains in the flue gas due to the excess combustion air. The flue gas composition is around 60% nitrogen, 37% water, a little under 3% oxygen and the rest is trace amounts of the other components. The carbon dioxide and nitric oxide contents are parts of these trace amounts, and the flue gas is therefore safe for release.

The flue gas contains 32 ppm of nitric oxide. This is an important gas for air pollution. It will oxidize to nitrogen dioxide in the atmosphere and can form acid rain. The content of nitric oxide is within the emission limit, as of the Norwegian Environment Agency (2020) [37].

Table 4.11 shows the temperature of the streams entering and exiting the boiler. It also shows the temperature of the combustion reaction.

Table 4.11: Temperatures of the boiler. The combustion temperature is the temperature at which the combustion occurs, which is given from Aspen Plus.

Stream	Temperature
Fuel	52.7 °C
Wet air	25 °C
Combustion	1700 °C
Flue gas	120 °C

Table 4.12 shows stream data for the streams in the steam producing loop. All streams are pure water.

Table 4.12: Data for the streams in the steam production loop. All streams are pure water.

	LP liquid	HP liquid	Steam
Temperature [°C]	50	50.6	184.5
Pressure [bar]	0.2	11	11
Vapor fraction	0	0	0.99
Mass flow [kg/h]	2072	2072	2072

The table shows that the boiler can produce 2072 kg/h of steam at the conditions wanted by NOAH. They have a need of around 6000 kg/h, which means that this alternative can cover approximately 1/3 of their steam demand.

A simple pinch analysis was performed to verify that the chosen flue gas temperature did not cause a temperature cross, and that the minimum temperature difference in the heat exchanger was kept above a minimum of 10 °C. A temperature cross or too small temperature difference will reduce the efficiency of the exchanger and give an unreasonably high exchanger area. If this had been the case, the temperature of the flue gas would have had to be changed to a higher temperature, which would have resulted in less usable heat. The pinch analysis is shown in Appendix C.2. The analysis showed that the minimum temperature difference is 70 °C, well above the minimum requirement of 10 °C.

4.2 Cost and sizing

4.2.1 Base case

Table 4.13 shows the cost of the equipment and the total cost of the base case. The reactor and the compressors are the major contributors. The cost of the reactor is as such a significant part of the cost of both Alternative 1 and Alternative 2 as well. Although, there are significant uncertainties related to the reactor cost. The volume of the reactor is based on several assumptions, see Appendix D.1. It is also possible that NOAH could modify the current tank, which acts as the reactor today. This would save costs related to the reactor, but is not necessarily feasible.

Table 4.13: Equipment and total cost of the base case with and without installation.

Equipment	Cost w/o inst. [MUSD]	Cost with inst. [MUSD]
Compressors	0.99	2.46
Heat exchangers	0.04	0.15
Separators	0.13	0.53
Reactor	1.15	2.88
Storage tank	0.48	1.93
Total	2.79	7.95

4.2.2 Alternative 1

Table 4.14 shows the design of the scrubber with data from the simulation in Aspen Plus and sizing using Aspen Process Economic Analyzer. The results shown in this table is used for the cost estimation of the scrubber.

Table 4.14: Case X and Case Y is the water scrubber at 1 bar and 35 bar respectively.

Parameter	Case X	Case Y
Diameter	0.3 m	0.15 m
Packing height	3.05 m	3.05 m
Packing volume	0.215 m^3	0.054 m^3
Vessel height	7.32 m	7.32 m
Vessel volume	0.517 m^3	0.129 m^3
Wall thickness	0.12 mm	2.13 mm
Shell mass	6.61 kg	58.78 kg

As described in Chapter 3 and Appendix D.1, there are several assumptions made, and consequently uncertainties, in the design of the scrubbers, which also lead to uncertainty in the cost estimation of the equipment. The cost of the scrubber is however expected to be a very small part of the total cost of the alternative, as especially the reactor and compressors generally are significantly more expensive equipment than a pressure vessel. An accurate cost estimation is not needed for reviewing the feasibility. The sizing and cost estimations are expected to be in the correct order of magnitude.

The packing height, and the scrubber height, are not expected to be equal for both scrubber configurations. The volume streams are significantly different, which would normally give different designs.

The shell masses given in Table 4.14 are below the minimum value given for the size parameter of the type of pressure vessel in Sinnott and Towler [25]. This leads to the accuracy of the cost to be low. The pressure vessel cost and sizing has an already high uncertainty due to the assumptions made for the diameter and height of the vessel. However, Table 4.16 shows that the cost of the scrubber is significantly smaller than the cost of the base case. The cost of the scrubber will therefore not affect the total cost to a large degree. A different method for calculating the cost should still be used in a more accurate analysis.

Table 4.15 shows the cost of the packing and the vessel of scrubber Case X and Y. Both cases are included to compare the cost increased by using a higher operating pressure. As described earlier, the sizing parameter for the packing is the volume of the packing in m^3, while the sizing parameter for the vessel is shell mass in kg. These parameters are used to estimate the costs shown in the table. The values of the sizing parameters are shown in

Table 4.14.

Table 4.15: Cost comparison of scrubber case X and Y. The cost of the vessel is given without installation.

	Case X [USD]	Case Y [USD]
Packing	530	130
Vessel	21100	23600

Table 4.15 shows that the increased operating pressure increases the cost with around 10%. This is a significant increase, but the increase in effectiveness of the cleaning due to the increased operating pressure is more important.

The packing cost included in Table 4.15 is presented as a one-time purchase. The packing will eventually have to be replaced, which will come with a cost. However, the cost of the packing is so low compared to the cost of the vessel that the cost of replacing the will not result in a significant change of the cost.

Table 4.16 shows the costs of alternative 1. The scrubber cost is the sum of the packing and vessel shown in Table 4.15. The scrubber cost are for Case Y, the water scrubber at 35 bar with a liquid-gas ratio of 3.5.

Table 4.16: Cost of Alternative 1. The scrubber cost is the sum of the packing and vessel cost for scrubber Case Y. The costs are given both without and with installation.

	Cost w/o inst.	Cost with inst.
Scrubber	23700 USD	94600 USD
Base case	2.79 MUSD	7.95 MUSD
Total cost	2.81 MUSD	8.04 MUSD

The scrubber increases the cost of the base case with 0.7% and 1.1% for the case without and with installation included respectively. This is a very small increase and not significant for the total cost of the project. This also shows that the assumptions used, and large uncertainties, for the sizing of the scrubber does not impact the total cost significantly.

Table 4.17 shows the production cost per kg produced hydrogen. The produced hydrogen is compressed, and cleaned for Alternative 1, and ready for

storage or utilization. The production costs given in the table are for a ten year horizon, meaning the amount of hydrogen produced over ten years. This is more relevant than showing data for a year, as the payment of expensive equipment are usually paid in installments over several years. The production cost is obtained by dividing the total cost of the case by the hydrogen production. The hydrogen production over the ten years is 1800 tons.

Table 4.17: Production cost per kg of produced hydrogen for the base case and Alternative 1 over ten years of operation. The hydrogen production over ten years is 1800 tons.

Case	Cost w/o inst.	Cost with inst.
Base case	1.5 USD/kgH_2	4.4 USD/kgH_2
Alternative 1	1.6 USD/kgH_2	4.5 USD/kgH_2

Table 4.17 shows, as in Table 4.16, that the inclusion of the scrubber does not add a significant increase in the cost of the product. The production cost only increase by 0.1 USD/kgH_2, and will not affect the feasibility of the project significantly.

4.2.3 Alternative 2

Table 4.18 shows the cost of the pump, the boiler, the reactor and the total cost of Alternative 2. The calculations for the costs are shown in Appendix D.2.

Table 4.18: Cost of the pump, the boiler, the reactor and the total cost of Alternative 2 with and without installation.

	Cost w/o inst. [MUSD]	Cost with inst. [MUSD]
Pump	0.01	0.05
Boiler	0.28	0.55
Reactor	1.15	2.88
Total cost	1.44	3.48

Table 4.18 shows that the reactor is the most significant cost of Alternative 2.

There is a significant uncertainty in this estimation as only the reactor, boiler and pump are included. There is, as mentioned, uncertainty tied to

the reactor sizing and cost, which could make a big impact on the estimated cost of the alternative. The estimation of the boiler cost is also uncertain, as an estimation for a furnace was used. Using data from Sinnott and Towler [25] for a boiler, but outside the boundaries of the size parameter, would however give a lower cost than the one shown in the table. Other equipment might be needed for the implementation of this alternative, in addition to a pipe system for the steam production. Operating cost for this alternative is also not included and will increase the cost of the project.

Table 4.19 shows the production cost of the steam for a one and ten year time period. The production cost is found by dividing the total cost of the project on the amount of steam produced in the given time period.

Table 4.19: Steam production cost for Alternative 2 for a one and ten year time period.

Steam production	Prod cost (1 year)	Prod cost (10 years)
7770 tons/year	0.45 USD/kg steam	0.045 USD/kg steam

4.2.4 Cost comparison

Table 4.20: Cost comparison of the alternatives.

Case	Cost w/o inst. [MUSD]	Cost with inst. [MUSD]
Base case	2.79	7.95
Alternative 1	2.81	8.04
Alternative 2	1.44	3.48

The comparison in Table 4.20 shows that Alternative 1 is around double the cost of Alternative 2. The majority of the cost of Alternative 1 comes from the base case, while the majority of Alternative 2 comes from the reactor.

4.3 Further discussion

As is expected from a preliminary assessment, there was made a set of assumptions in the equipment sizing that can provide a negative impact on the accuracy of the cost estimation. If the project is to be continued, a more in-depth analysis would have to be performed. All of the equipment involves significant uncertainties, as well as the method for estimating them. Sinnott and Towler's method gives an estimate, but is not accurate due to

among others the variability in equipment for different purposes. The cost estimation used for this project is also mostly based on the purchase cost of the different equipment and their installation cost. Operating costs may add a significant increase in the cost, but many of them are already covered as the implementation of the alternatives would be at an existing plant. The inflation is based on values for summer 2021, which may also change rapidly.

The proposed route of Alternative 1 did not reach the required hydrogen fuel quality for PEMFCs according to *ISO 14687*. However, the composition could be suitable for SOFCs, as they are less sensitive to impurities as they can handle a wider range of fuels. This would need further investigation. This change would lower the purification requirement of the hydrogen gas, which gives a lowered cost. This would however depend on the choice of application that is wanted at the company. SOFCs are not applicable for vehicle applications due to the high operating temperature, and not having the power density and compactness of the PEMFCs. However, if stationary power production is chosen, SOFCs might be a good alternative. With this application, the size of the fuel cells are not such an important factor, and with their high efficiency and better handling of impurities, SOFCs could prove better than PEMFCs.

A possible improvement for Alternative 1 would be to study different operating conditions that would avoid the formation of problematic impurities. Unfortunately, this path seems unfeasible, as it could promote negative consequences related to the gypsum production and the reactor configuration. As mentioned before, the ash comes from different sources and its composition vary from shipment to shipment, which hinders a better understanding of the ash composition.

From the cost comparison in Table 4.20 it is shown that Alternative 1: Fuel cells require two times the investment of Alternative 2: Process heat production. Alternative 1 will in addition be even more expensive when adding the cost of the fuel cells, which are not included in this preliminary study. Based on data from NOAH, they are expected to add an additional cost in the order of one million USD. Alternative 2 is therefore a significantly cheaper alternative.

However, the current production cost for Alternative 1 at 4.5 USD/kgH_2, is comparable to values from the open literature. Figure 4.1, presented by Hassan et al.[38], shows that the production cost is higher than most of the production methods from non-renewables, but lower than most methods utilizing renewable hydrogen. The values are comparable with those from

Kannah et al.[8], Yanez et al.[1] and the Hydrogen Council[10] among others. Kannah et al. also adds that hydrogen could potentially unlock 8% of the global energy demand with a hydrogen production cost of 2.5 USD/kg.

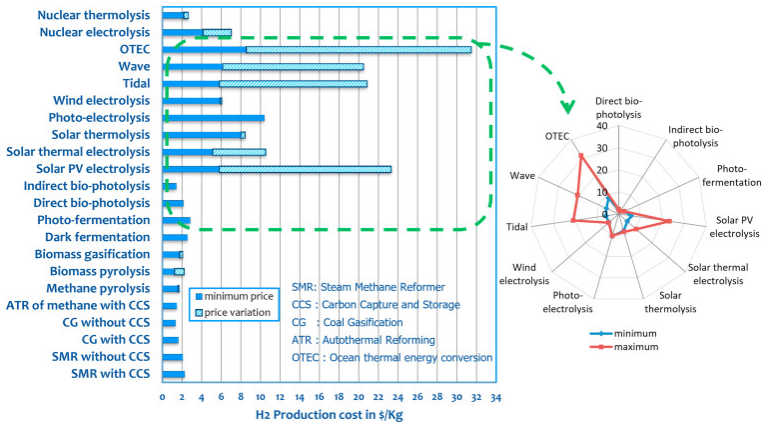

Figure 4.1: Production cost of hydrogen for some production methods.[38]

Comparatively, Alternative 2 has a production cost of steam at 0.045 USD/kg steam for a ten year period. Compared to the open literature, which presents a cost of 0.011[39] USD/kg steam, the cost is significantly higher. Additionally, the cost of this project does not include among others operating costs, as discussed earlier, so the production cost would in reality be even higher.

Alternative 1 would probably be more difficult to implement than Alternative 2. In addition to the setup described in this project, it would require implementation of the fuel cells, or possible a filling station if it would be used as fuel. Alternative 2 would be easier to implement as the setup for using steam in the *Resalt* project is already planned. Transport and collection of the hydrogen gas before combustion would although still need to be addressed.

Alternative 1 would in addition require more cleaning than the scrubber could provide, as the carbon monoxide, and water, levels are still too high for usage in PEMFCs. On the other hand, the steam or the flue gas does not need any treatment before it could be used in Alternative 2.

Due to the high purity of hydrogen in the process stream, the choice of Alternative 2 provides a controversial aspect related to the implementation of greener technologies. Alternative 1 fits the green shift scenario better.

Both alternatives would be a good way for NOAH to save costs and be a

little greener. Alternative 1 could provide a good amount of power than can be utilized on-site, while Alternative 2 could cover around 1/3 of the steam demand of the *Resalt* project at NOAH. This means that both alternatives show potential related to application, but also to a degree with regards to the economics of the alternatives.

The production cost would although probably be higher than the literature when all costs which are currently not accounted for are included. At the same time, NOAH does not plan to sell the hydrogen or the steam, but to use it on-site. This means that the price does not need to be extremely competitive with other production methods, but rather around the same level to justify the on-site application for saving other costs and the environment.

Chapter 5

Conclusion

This thesis presents an investigation into different opportunities for application of hydrogen produced from MSWI fly ash, in cooperation with the company NOAH. The objective was look into two main alternatives for application: purification for usage in fuel cells for power production and process heat production from combustion of the gas stream. The feasibility of the alternatives were studied and compared. Utilization of hydrogen as an energy carrier is a topic gaining momentum in the energy sector, and it has potential to replace parts of the non-renewable sources that are utilized today. Implementing hydrogen as a resource for NOAH could be a beneficial possibility for the company and the environment.

Alternative 1 describes a process of producing, compression, purifying and storage of the hydrogen, with the purpose of being utilized in fuel cells. Fuel cells require a high purity level for hydrogen, and removal of contaminants is very important to ensure efficient use. *ISO 14687* presents the required purity level and contamination limits for PEM fuel cells, which was used for comparison in this project. Scrubbing with water and sodium hydroxide were the investigated cleaning methods for the gas in this project. Several scrubber configurations were investigated, and water scrubbing operating at 35 bar with a liquid-gas ratio of 3.5 was found to be most efficient.

The purified and compressed hydrogen was found to have a high enough hydrogen content for utilization in fuel cells. The simulations showed complete removal of most problematic impurities, while the water and carbon monoxide levels still were above the required limit. The water removal is considered to be less of an issue than the carbon monoxide. Sufficient water

removal might be reached by reducing the temperature of the intercooling, or other changes to the configuration of the compressors, heat exchangers or separators. However, carbon monoxide would have to be targeted by the inclusion a specific removal technology for this contaminant. The contamination problem could be solved by the usage of a different type of fuel cell, for instance solid oxide fuel cells. This type handles impurities better than PEM fuel cells, but can only be used for stationary applications, not for vehicles, and require a high operating temperature.

The total cost of Alternative 1 was estimated to 2.81 MUSD and 8.04 MUSD without and with installation, respectively. The cost of the reactor and compressors are the major contributors to the cost, as for the base case. The inclusion of the cleaning method increased the cost by only around 1% compared to the cost of the base case. The production cost of hydrogen for Alternative 1 was estimated to be 4.5 USD/kgH_2 for a ten year operating period, which is comparable to production costs from the open literature. The studied case was found to be especially competitive with hydrogen production methods from renewable sources.

Alternative 2 describes the combustion of the hydrogen gas stream and utilizing the produced heat for steam production. NOAH has another ongoing project where this steam could be used. This application would remove the need for purification, compression and storage. The reactor would still be required as in Alternative 1, and a boiler would also be needed. The flue gas of the combustion has a composition of around 60% nitrogen, around 37% water and around 3% oxygen, with the remaining being trace amount of carbon dioxide, carbonyl sulfide, nitric oxide and phosphine.

This process was found to be producing 1.54 MW. For comparison, this is enough to cover the yearly energy demand of around 270 Norwegian households. The steam production of around 2070 kg/h was found to be able to cover around 1/3 of the steam demand of NOAH.

The total cost of Alternative 2 was estimated to be 1.44 MUSD and 3.48 MUSD without and with installation, respectively. The reactor is the major contributor to the cost. The production cost of the steam was estimated to be 0.045 USD/kg steam over a ten year time period. This is significantly higher than steam costs found in the open literature.

Alternative 2 was found to be around half the investment of Alternative 1. However, Alternative 1 provides a similar production cost to the open literature, while the steam production cost of Alternative 2 is significantly

higher than the literature. The objective of the hydrogen is not to be sold, and as such, the production cost does not need to be highly competitive with other methods. They should still to a degree be comparable to justify the application.

This work has presented a preliminary study of the feasibility and opportunities of the small scale hydrogen production at NOAH. There has been made a set of assumptions for the estimations which lead to uncertainties related to the cost estimation. The small scale of the case made it difficult to find valid correlations and comparisons. In addition, operating costs were not included. A more in-depth investigation with much more precise sizing and cost estimation would have to be performed before implementing and utilize any of the alternatives. Still, at this stage, both alternatives show potential of being real possibilities as an application for the hydrogen, for saving costs related to energy and process utilities, and the environment.

5.1 Future work

The hydrogen gas stream of Alternative 1 is still not pure enough for use in PEM fuel cells. The content of water, and more importantly carbon monoxide, are above the concentration limit. Technology for removal of carbon monoxide is therefore in need of investigation to find an applicable technology for this case. Additional removal of water is also needed. An investigation of other configurations for the compressors, intercooling and separators could be done to see if this could remove enough water for the required standard.

A deeper investigation into the utilization of SOFCs instead of PEMFCs should be done. SOFCs can, as mentioned, handle impurities better, but requires a higher operating temperature and is not suited for mobile applications. For power generation on-site, this type could prove to be better suited than PEMFCs.

For this project, there was a desire to investigate the usage of pressure swing adsorption (PSA) and membranes for the purification. PSA is the most utilized method for hydrogen purification and it would be interesting to see if this purification method could reach the fuel cell standard alone. Membranes, for instance Pd-membranes, with high hydrogen selectivity, would also be interesting to investigate in more detail. These can reach very high hydrogen purity and should be able to satisfy the fuel cell standard. However, these can be very costly and membranes is still a field in development.

Both these purification methods, and potentially others, should be investigated as they can be more effective and/or cheaper to implement in a small scale case as the one that was studied. The scrubber configurations could also be looked further into, to find an even more optimized scrubber.

A more in-depth cost estimation, with more accurate sizing, is needed for the continuation of this investigation and to decide its feasibility. This is required for all equipment as there is much uncertainty for all estimations. Operating cost and other expenses, such as the fuel cells of Alternative 1, need to be included. The fuel cells in particular will add a significant increase for the alternative. This is needed to be able to compare the different alternatives for application, and decide what is most applicable for the objective of NOAH.

A sensitivity analysis for variations in the produced amount of hydrogen should be performed. A change in the production could impact the competitiveness significantly. A sensitivity analysis and deeper investigation into the reactor configuration should also be performed. Possible parameters to study include the reactor temperature and the ash/water ratio. This could both lead to increased production with lower impurity levels, as well as to save costs.

Bibliography

[1] M. Yáñez, F. Relvas, A. Ortiz, D. Gorri, A. Mendes, and I. Ortiz, "Psa purification of waste hydrogen from ammonia plants to fuel cell grade," *Separation and Purification Technology*, vol. 240, p. 116334, 2020.

[2] F. Dawood, M. Anda, and G. Shafiullah, "Hydrogen production for energy: An overview," *International Journal of Hydrogen Energy*, vol. 45, no. 7, pp. 3847–3869, 2020.

[3] D. Gielen, F. Boshell, D. Saygin, M. D. Bazilian, N. Wagner, and R. Gorini, "The role of renewable energy in the global energy transformation," *Energy Strategy Reviews*, vol. 24, pp. 38–50, 2019.

[4] C.-F. Schleussner, "*The Paris Agreement - the 1.5℃ Temperature Goal.*" Accessed at `https://climateanalytics.org/briefings/15c/`, June 2022.

[5] A. Abdeljaoued, F. Relvas, A. Mendes, and M. H. Chahbani, "Simulation and experimental results of a psa process for production of hydrogen used in fuel cells," *Journal of Environmental Chemical Engineering*, vol. 6, no. 1, pp. 338–355, 2018.

[6] A. Arregi, M. Amutio, G. Lopez, J. Bilbao, and M. Olazar, "Evaluation of thermochemical routes for hydrogen production from biomass: A review," *Energy Conversion and Management*, vol. 165, pp. 696–719, 2018.

[7] J. Rajesh Banu, S. Kavitha, R. Yukesh Kannah, R. R. Bhosale, and G. Kumar, "Industrial wastewater to biohydrogen: Possibilities towards successful biorefinery route," *Bioresource Technology*, vol. 298, p. 122378, 2020.

[8] R. Yukesh Kannah, S. Kavitha, Preethi, O. Parthiba Karthikeyan, G. Kumar, N. V. Dai-Viet, and J. Rajesh Banu, "Techno-economic

assessment of various hydrogen production methods – a review," *Bioresource Technology*, vol. 319, p. 124175, 2021.

[9] Z. Du, C. Liu, J. Zhai, X. Guo, Y. Xiong, W. Su, and G. He, "A review of hydrogen purification technologies for fuel cell vehicles," *Catalysts*, vol. 11, no. 3, 2021.

[10] Hydrogen Council, "*Path to Hydrogen Competitiveness: A Cost Perspective*." (2020) Accessed: `https://hydrogencouncil.com/wp-content/uploads/2020/01/Path-to-Hydrogen-Competitiveness_Full-Study-1.pdf`, 2021.

[11] IEA, "*Global demand for pure hydrogen, 1975-2018*." IEA, Paris. Accessed at `https://www.iea.org/data-and-statistics/charts/global-demand-for-pure-hydrogen-1975-2018`, June 2022.

[12] J. P. Flem, "*Techno-Economic Assessment of Hydrogen Production from CFB ash*." Specialization project report. Department of Chemical Engineering NTNU, December 17, 2021.

[13] NOAH, "*About NOAH*." Accessed: `https://en.noah.no/our-business/about-noah/our-business-2/`, June 2022.

[14] U.S. Department of Energy, "*Reaction of Aluminum with Water to Produce Hydrogen*." 2008.

[15] R. O'hayre, S.-W. Cha, W. Colella, and F. B. Prinz, *Fuel cell fundamentals*. John Wiley & Sons, 2016.

[16] S. Mekhilef, R. Saidur, and A. Safari, "Comparative study of different fuel cell technologies," *Renewable and Sustainable Energy Reviews*, vol. 16, no. 1, pp. 981–989, 2012.

[17] International Organization for Standardization, "*Hydrogen fuel quality - Product Specification*." ISO 14687:2019(E).

[18] O. Z. Sharaf and M. F. Orhan, "An overview of fuel cell technology: Fundamentals and applications," *Renewable and Sustainable Energy Reviews*, vol. 32, pp. 810–853, 2014.

[19] I. Bionomic Industries, "*Series 5000 Packed Tower Fume Scrubber and Air Stripper*." Accessed at `https://www.bionomicind.com/wet-scrubbers/5000-fume-scrubber.cfm`, June 2022.

[20] M. Zhao, P. Xue, J. Liu, J. Liao, and J. Guo, "A review of removing so2 and nox by wet scrubbing," *Sustainable Energy Technologies and Assessments*, vol. 47, p. 101451, 2021.

[21] H. M. A. Sharif, N. Mahmood, S. Wang, I. Hussain, Y.-N. Hou, L.-H. Yang, X. Zhao, and B. Yang, "Recent advances in hybrid wet scrubbing techniques for nox and so2 removal: State of the art and future research," *Chemosphere*, vol. 273, p. 129695, 2021.

[22] S. SIRCAR and T. C. GOLDEN, "Purification of hydrogen by pressure swing adsorption," *Separation Science and Technology*, vol. 35, no. 5, pp. 667–687, 2000.

[23] D. D. Papadias, S. Ahmed, R. Kumar, and F. Joseck, "Hydrogen quality for fuel cell vehicles – a modeling study of the sensitivity of impurity content in hydrogen to the process variables in the smr–psa pathway," *International Journal of Hydrogen Energy*, vol. 34, no. 15, pp. 6021–6035, 2009.

[24] A. Golmakani, S. Fatemi, and J. Tamnanloo, "Investigating psa, vsa, and tsa methods in smr unit of refineries for hydrogen production with fuel cell specification," *Separation and Purification Technology*, vol. 176, pp. 73–91, 2017.

[25] R. Sinnott and G. Towler, *Chemical Engineering Design*. Butterworth-Heinemann, 6th ed., 2020.

[26] N. Al-Mufachi, N. Rees, and R. Steinberger-Wilkens, "Hydrogen selective membranes: A review of palladium-based dense metal membranes," *Renewable and Sustainable Energy Reviews*, vol. 47, pp. 540–551, 2015.

[27] M. A. Fahim, T. A. Alsahhaf, and A. Elkilani, *Chapter 11 - Hydrogen Production*. Amsterdam: Elsevier, 2010.

[28] I. Q. Search, "*Steam Boilers*." Accessed at `https://www.iqsdirectory.com/articles/boiler/steam-boilers.html`, June 2022.

[29] Store Norske Leksikon, "*hydrogen*." Accessed at `https://snl.no/hydrogen`, December 2021.

[30] NOAH, "*Breakthrough in salt recovery*." Accessed: `https://en.noah.no/breakthrough-in-salt-recovery/`, June 2022.

[31] A. Kayode Coker, *Ludwig's Applied Process Design for Chemical and Petrochemical Plants*. Elsevier, 4th ed., 2015.

[32] "Chemical engineering plant cost index." `https://www.chemengonline.com/pci`.

[33] "*Elektrisitetpriser*." Retreieved from `https://www.ssb.no/energi-og-industri/energi/statistikk/elektrisitetspriser`, December 2021.

[34] "*Valutakalulator*." Retreieved from `https://www.dnb.no/markets/valuta-og-renter/valutakalkulator`, December 2021.

[35] Engineering ToolBox, "*Solubility of Gases in Water vs. Temperature*." (2008) Accessed at `https://www.engineeringtoolbox.com/gases-solubility-water-d_1148.html`, 13th May 2022.

[36] "*Energibruk i husholdningene*." Retrieved from `https://www.ssb.no/energi-og-industri/energi/statistikk/energibruk-i-husholdningene`, May 2022.

[37] B. N. AS, "*Tillatelse etter forurensningsloven for produksjon og drift på Skarvfeltet*." Permit together with the Norwegian Environment Agency, 2020.

[38] I. Hassan, H. S. Ramadan, M. A. Saleh, and D. Hissel, "Hydrogen storage technologies for stationary and mobile applications: Review, analysis and perspectives," *Renewable and Sustainable Energy Reviews*, vol. 149, p. 111311, 2021.

[39] R. Yukesh Kannah, S. Kavitha, Preethi, O. Parthiba Karthikeyan, G. Kumar, N. V. Dai-Viet, and J. Rajesh Banu, "Techno-economic assessment of various hydrogen production methods – a review," *Bioresource Technology*, vol. 319, p. 124175, 2021.

[40] David R. Lide, *CRC Handbook of Chemistry and Physics*. CRC Press, 85th ed., 2004. pp. 6-8.

[41] Engineering ToolBox, "*Water Vapor - Specific Heat vs. Temperature*." (2005) Accessed at `https://www.engineeringtoolbox.com/water-vapor-d_979.html`, 28th May 2022.

[42] Engineering ToolBox, "*Nitrogen - Specific Heat vs. Temperature.*" (2005) Accessed at `https://www.engineeringtoolbox.com/nitrogen-d_977.html`, 28th May 2022.

[43] Engineering ToolBox, "*Oxygen - Specific Heat vs. Temperature.*" (2005) Accessed at `https://www.engineeringtoolbox.com/oxygen-d_978.html`, 28th May 2022.

[44] Engineering ToolBox, "*Water - Specific Heat vs. Temperature.*" (2004) Accessed at `https://www.engineeringtoolbox.com/specific-heat-capacity-water-d_660.html`, 28th May 2022.

[45] Engineering ToolBox, "*Saturated Steam - Properties for Pressure in Bar.*" (2003) Accessed at `https://www.engineeringtoolbox.com/saturated-steam-properties-d_457.html`, 29th May 2022.

[46] L. Gracia, P. Casero, C. Bourasseau, and A. Chabert, "Use of hydrogen in off-grid locations, a techno-economic assessment," *Energies*, vol. 11, no. 11, 2018.

[47] T. Hua, R. Ahluwalia, J.-K. Peng, M. Kromer, S. Lasher, K. McKenney, K. Law, and J. Sinha, "Technical assessment of compressed hydrogen storage tank systems for automotive applications," *International Journal of Hydrogen Energy*, vol. 36, no. 4, pp. 3037–3049, 2011.

[48] H. T. Hwang and A. Varma, "Hydrogen storage for fuel cell vehicles," *Current Opinion in Chemical Engineering*, vol. 5, pp. 42–48, 2014. Energy and environmental engineering / Reaction engineering.

[49] M. Paster, R. Ahluwalia, G. Berry, A. Elgowainy, S. Lasher, K. McKenney, and M. Gardiner, "Hydrogen storage technology options for fuel cell vehicles: Well-to-wheel costs, energy efficiencies, and greenhouse gas emissions," *International Journal of Hydrogen Energy*, vol. 36, no. 22, pp. 14534–14551, 2011. Fuel Cell Technologies: FUCETECH 2009.

[50] J. M. Bellosta von Colbe, G. Lozano, O. Metz, T. Bücherl, R. Bormann, T. Klassen, and M. Dornheim, "Design, sorption behaviour and energy management in a sodium alanate-based lightweight hydrogen

storage tank," *International Journal of Hydrogen Energy*, vol. 40, no. 7, pp. 2984–2988, 2015.

[51] Cumalioglu I. and Ma Y. and Ertas A. and Maxwell T., "High pressure hydrogen storage tank: A parametric design study.," *J. Pressure Vessel Technol.*, pp. 216–222, 2007.

Appendix A

Stream data

A.1 Stream data from scrubber simulations

Table A.1, A.2 and A.3 show stream data for the gas in- and outflow for the water scrubbers with an L/G of 2.1 at 1 bar, 11 bar and 35 bar respectively. Table A.6 and A.7 show the data for the water scrubbers at 1 bar and 35 bar respectively at increased L/G ratios of 10.4 and 3.5 respectively. Table A.4 and A.5 show the same data for the NaOH scrubbers at 11 bar and 35 bar respectively.

Table A.1: Stream data for scrubber case A.

Component	Inlet [kmol/h]	Outlet [kmol/h]	Outlet mole fraction	Removed [%]
H2	24.7595	24.7595	0.9797	5.6E-08
H2O	0.4333	0.5107	0.0202	-17.86
CO	5.0E-05	5.0E-05	2.0E-06	0.06
CO2	3.2E-05	1.5E-24	6.1E-26	100
COS	1.1E-06	1.1E-06	4.4E-08	2.96
NH3	0.0022	0,0012	4,6E-05	47.55
CH4	0.0019	0.0019	7.4E-05	0.46
Total	25.20	25.27	-	-

As described in Chapter 3, additional simulations were run for the water scrubbers at 1 bar and 35 bar at an increased liquid-gas ratio, L/G. The results for the scrubber at 1 bar with an L/G of 10.4, Case X, is shown in

Table A.2: Stream data for scrubber case B.

Component	Inlet [kmol/h]	Outlet [kmol/h]	Outlet mole fraction	Removed [%]
H2	24.7595	24.7595	0.9978	6.0E-07
H2O	0.0434	0.0538	0.0022	-23.91
CO	5.0E-05	4.9E-05	2.0E-06	0.55
CO2	3.2E-05	8.5E-20	3.4E-21	100
COS	1.1E-06	8.4E-07	3.4E-08	26.66
NH3	0.0020	5.8E-13	2.4E-14	100.00
CH4	0.0019	0.0018	7.3E-05	4.30
Total	24.81	24.82	-	-

Table A.3: Stream data for scrubber case C.

Component	Inlet [kmol/h]	Outlet [kmol/h]	Outlet mole fraction	Removed [%]
H2	24.7595	24.7595	0.9992	1.8E-06
H2O	0.0144	0.0181	0.0007	-25.72
CO	5.0E-05	4.9E-05	2.0E-06	1.61
CO2	3.2E-05	8.2E-19	3.3E-20	100
COS	1.1E-06	2.7E-07	1.1E-08	76.61
NH3	0.0019	3.4E-21	4.8E-23	100
CH4	0.0019	0.0016	6.7E-05	12.44
Total	24.78	24.78	-	-

Table A.6 and the results for the water scrubber at 35 bar with an L/G of 3.5, Case Y, is shown in Table A.7.

Table A.8 shows the mole fraction of the cleaned gas after scrubbing.

A.2 Additional stream data

A.2.1 Mole fractions base case

Table A.9 shows the mole fractions of the in- and outflow of the compression train, in addition to the streams after each of the five compressions.

Table A.4: Stream data for scrubber case D.

Component	Inlet [kmol/h]	Outlet [kmol/h]	Outlet mole fraction	Removed [%]
H2	24.7595	24.7595	0.9979	2.4E-07
H2O	0.0434	0.0490	0.0020	-12.86
CO	5.0E-05	4.9E-05	2.0E-06	0.22
CO2	3.2E-05	3.6E-29	1.5E-30	100
COS	1.1E-06	1.0E-06	4.1E-08	10.58
NH3	0.0020	0.0008	3.1E-05	62.02
CH4	0.0019	0.0018	7.5E-05	1.71
Total	24.81	24.81	-	-

Table A.5: Stream data for scrubber case E.

Component	Inlet [kmol/h]	Outlet [kmol/h]	Outlet mole fraction	Removed [%]
H2	24.7595	24.7595	0.9993	7.4E-07
H2O	0.0144	0.0164	0.0007	-14.05
CO	5.0E-05	4.9E-05	2.0E-06	0.64
CO2	3.2E-05	1.2E-29	4.9E-31	100
COS	1.1E-06	7.8E-07	3.2E-08	31.18
NH3	0.0019	1.7E-06	7.0E-08	99.91
CH4	0.0019	0.0018	7.2E-05	4.96
Total	24.78	24.78	-	-

A.2.2 Alternative 2: Process heat production

Table A.10 shows stream data for the cooling water used in the heat exchanger to illustrate the usage of the steam.

Table A.6: Stream data for scrubber case X.

Component	Inlet [kmol/h]	Outlet [kmol/h]	Outlet mole fraction	Removed [%]
H2	24.7595	24.7595	0.9766	2.9E-07
H2O	0.4333	0.5910	0.0233	-36.38
CO	5.0E-05	4.9E-05	2.0E-06	0.30
CO2	3.2E-05	2.5E-19	1.0E-20	100
COS	1.1E-06	9.7E-07	3.8E-08	14.69
NH3	0.0022	5.7E-08	2.3E-09	100
CH4	0.0019	0.0018	7.3E-05	2.29
Total	25.20	25.35	-	-

Table A.7: Stream data for scrubber case Y.

Component	Inlet [kmol/h]	Outlet [kmol/h]	Outlet mole fraction	Removed [%]
H2	24.7595	24.7595	0.9992	3.1E-06
H2O	0.0144	0.0181	0.0007	-26.00
CO	5.0E-05	4.8E-05	2.0E-06	2.67
CO2	3.2E-05	2.6E-19	1.0E-20	100
COS	1.1E-06	2.0E-08	8.1E-10	98.24
NH3	0.0019	5.1E-31	2.1E-32	100
CH4	0.0019	0.0015	6.0E-05	20.71
Total	24.78	24.78	-	-

Table A.8: Composition of the cleaned gas stream after the scrubbing for the different configurations. The composition is given as a mole fraction.

	Case A	Case B	Case C	Case D	Case E
H2	0.9797	0.9978	0.9992	0.9979	0.9993
H2O	0.0202	0.0022	0.0007	0.0020	0.0007
CO	2.0E-06	2.0E-06	2.0E-06	2.0E-06	2.0E-06
CO2	6E-26	3E-21	3E-20	1E-30	5E-31
COS	4.4E-08	3.4E-08	1.1E-08	4.1E-08	3.2E-08
NH3	4.6E-05	2E-14	5E-23	3.1E-05	7.0E-08
CH4	7.4E-05	7.3E-05	6.7E-05	7.5E-05	7.2E-05

Table A.9: Mole fractions of the streams in the base case. The inflow stream is the inflow to the compression train which is the outlet flow of the reactor. The outflow is the hydrogen gas product stream. The remaining streams are the post compression streams for each compressor.

Comp	Inflow	C101	C102	C103	C104	C105	Outflow
H2	0.8883	0.9826	0.9944	0.9981	0.9993	0.9996	0.9996
H2O	0.1115	0.0172	0.0055	0.0017	0.0006	0.0002	0.0002
NH3	9.2E-05	8.8E-05	8.4E-05	8.1E-05	7.7E-05	7.4E-05	7.4E-05
CO	1.8E-06	2.0E-06	2.0E-06	2.0E-06	2.0E-06	2.0E-06	2.0E-06
CO2	1.2E-06	1.3E-06	1.3E-06	1.3E-06	1.3E-06	1.3E-06	1.3E-06
COS	4.1E-08	4.5E-08	4.6E-08	4.6E-08	4.6E-08	4.6E-08	4.6E-08
CH4	6.8E-05	7.5E-05	7.6E-05	7.6E-05	7.6E-05	7.6E-05	7.6E-05
PH3	5.3E-07	5.9E-07	5.9E-07	6.0E-07	6.0E-07	6.0E-07	6.0E-07
N2O	8.8E-06	9.7E-06	9.9E-06	9.9E-06	9.9E-06	9.9E-06	9.9E-06

Table A.10: Stream data for the cooling water used for the heat exchanger of the steam loop. The heat exchanger simulates the utilization of the steam. The streams are pure liquid water.

	Cold in	Cold out
Temperature	20 °C	116.9 °C
Pressure	11 bar	11 bar
Mass flow	12600 kg/h	12600 kg/h

Appendix B

Hydrogen production

B.1 Water content of reactor outflow

The calculation of the water content of the reactor flow was performed in the previous work[12]. A shortened version of the calculation will be presented here.

As the fraction of the impurities are so small, the reactor outstream was assumed to contain only hydrogen and water for this calculation. The hydrogen mass flow was assumed to be 50 kg/h. The gas stream was assumed to be saturated with water, so the saturation vapor pressure of water is used in the calculations. As the temperature of the outstream is assumed to be at 50 °C, the saturation pressure for this temperature is used. The value is from *CRC Handbook of Chemistry and Physics*[40].

$$p^{sat}_{H_2O}(50\,^{\circ}\mathrm{C}) = 12.3\,\mathrm{kPa}$$

The partial pressure for hydrogen was then found. The total pressure of the stream exiting the reactor is assumed to be 1.1 bar. The total pressure can be given as the sum of the partial pressures of the components, see Equation B.1.1.

$$p_{tot} = p_{H2} + p^{sat}_{H_2O}(50\,^{\circ}\mathrm{C}) \tag{B.1.1}$$

Under the assumption of ideal gas, the ratio between the partial pressures of

the components will be the same as the ratio between the number of moles. The ratio between the moles of hydrogen and water can then be found by

$$\frac{n_{H2}}{n_{H2O}} = \frac{p_{H2}}{p^{sat}_{H_2O}(50\,^\circ\mathrm{C})} \tag{B.1.2}$$

By using the known mass flow of hydrogen, molar mass of hydrogen and of water the mass flow of water is found to be

$$\dot{m}_{H2O} = 15.74\,\mathrm{g/s} \tag{B.1.3}$$

Appendix C

Combustion

C.1 Composition of combustion air

This calculation was performed before setting up the simulation of Alternative 2 to determine the composition of the combustion air with the current assumptions.

As described earlier the fuel is assumed to consist of 50 kg/h hydrogen, including impurities, and 56.7 kg/h of water. The molecular mass of a hydrogen molecule is 2 g/mol and 18 g/mol for water. Using Equation C.1.1 the mole flows of hydrogen and water in the fuel are found.

$$\dot{n} = \frac{\dot{m}}{M} \tag{C.1.1}$$

where $\dot{n}$ is the mole flow, $\dot{m}$ is the mass flow and M is the molecular mass. From Equation 3.4.3, one mole of oxygen is required per two moles of hydrogen for stoichiometric combustion. The required amount of oxygen for stoichometric combustion of the fuel stream is then found by dividing the hydrogen mole flow by two. The required mole flow of oxygen, as well as the mole flow of water and hydrogen in the fuel, are shown in Table C.1.

20% excess air was used for the calculation for ensuring complete combustion as described in Chapter 2.

The oxygen content with excess is calculated by multiplying the stoichiometric oxygen content with $1+20/100 = 1.2$. The oxygen mole flow is shown in Table 3.5.

Table C.1: Mole flows of hydrogen and water in the fuel, and required oxygen for stoichiometric combustion.

	Mole flow
Hydrogen in fuel	25.0 kmol/h
Water in fuel	3.2 kmol/h
Required oxygen	12.5 kmol/h

The ratio of nitrogen and oxygen in the air is $78/21 = 3.71$. The nitrogen content with excess air is then calculated by multiplying the ratio with the mole flow of oxygen. The nitrogen flow is shown in Table 3.5.

The water content of the wet air is calculated as follows. The saturation pressure for water at 50 °C is 0.123 bar[40]. With an assumed 80% moisture content in the air, the partial pressure of water, p_{H2O}, in the air is $0.8 \cdot 0.123$ which gives 0.098 bar. The ratio of water/air is then given by Equation C.1.2. The pressure of the air stream, p_{tot} is assumed to be 1.1 bar.

$$\begin{aligned} \frac{n_{H2O}}{n_{air}} &= \frac{p_{H2O}}{p_{tot} - p_{H2O}} = \frac{0.098}{1.1 - 0.098} \\ &= 0.098 \end{aligned} \tag{C.1.2}$$

The water content is then found by multiplying the water/air ratio with the amount of air. The mole flows for the components of the air are shown in Table C.2. This table is also included in Chapter 3.

Table C.2: Mole flows of the wet air for the combustion, with 20% excess air and 80% moisture.

Component	Mole flow
Oxygen	15.0 kmol/h
Nitrogen	55.7 kmol/h
Water	6.9 kmol/h

C.2 Pinch analysis for the boiler

This appendix shows the pinch analysis that was performed for the boiler as described in Chapter 4. The duty of the streams connected to the boiler was

calculated and used to perform the analysis. The streams are the fuel gas stream, from 1700 °C to 120 °C, the heating of water from 50 °C to 185 °C and the evaporation of the water at 185 °C, which is the boiling point for water at 11 bar.

As the specific heat is dependent on the temperature an average was calculated, as of Equation C.2.1 This gives a good enough value for the purpose of this analysis.

$$Cp_{av} = \frac{Cp_{high} + Cp_{low}}{2} \tag{C.2.1}$$

where Cp_{high} and Cp_{low} are the specific heat of the component at the highest and lowest temperature of the stream respectively.

Specific heat at the start and end temperature point for the major components of the flue gas are shown in Table C.3. These three components make up > 99 mole% of the flue gas. The average specific heat over the temperature interval is also shown for all components, calculated using Equation C.2.1.

Table C.3: Specific heat of the significant components of the flue gas [41] [42] [43]. Cp_{high} 1727 °C (2000 K). Cp_{low} is given for 127 °C (400 K)

Component	Cp_{high}	Cp_{low}	Cp_{av}
Water	2.836 kJ/kgK	1.901 kJ/kgK	2.369 kJ/kgK
Nitrogen	1.284 kJ/kgK	1.044 kJ/kgK	1.164 kJ/kgK
Oxygen	1.181 kJ/kgK	0.941 kJ/kgK	1.061 kJ/kgK

The specific heat of vapor and liquid water for the temperatures used in the pinch analysis are shown in Table C.4.

Table C.4: Specific heat of water vapor and liquid at specified temperature [41] [44].

State	Temperature	Cp
Vapor	177 °C (400 K)	1.9261 kJ/kgK
Liquid	177 °C (400 K)	4.43 kJ/kgK
Liquid	50 °C (323 K)	4.18 kJ/kgK

The enthalpies used to calculate the heat duty for the evaporation of water at 185 °C are shown in Table C.5.

Table C.5: Enthalpies for steam and liquid water at 185 °C[45]. The enthalpy difference is also shown.

	Enthalpy
Steam	2779.66 kJ/kg
Liquid	781.11 kJ/kg
Δh	1998.55 kJ/kg

Equation C.2.2 shows how the heat duty of the fuel gas stream and for the heating of the liquid water. Equation C.2.3 shows the heat for the evaporation.

$$q = \frac{\dot{m}}{3600\,\text{s/h}} \cdot C_p \cdot (T_{high} - T_{low}) \tag{C.2.2}$$

$$q = \frac{\dot{m}}{3600\,\text{s/h}} \cdot (h_{steam}(185\,^\circ\text{C}) - h_{liquid}(185\,^\circ\text{C})) \tag{C.2.3}$$

where q is the heat duty, T_{high} and T_{low} are the highest and lowest temperature of the stream, and $\dot{m}$ is the mass flow of water from the steam producing loop in the simulation in Aspen Plus at 2072 kg/h, from Table 4.12. $h_{steam}(185\,^\circ\text{C})$ and $h_{liquid}(185\,^\circ\text{C})$ are the enthalpies of steam and liquid water at 185 °C given in Table C.5.

Table C.6 shows the heat duty of each of the streams used to draw the pinch diagram showed in Figure C.1. The value for the fuel gas stream is close to the produced heat duty given in Aspen Plus of 1.54 MW, and shows that the calculation using Equation C.2.2 and C.2.3 gives reasonable values.

Table C.6: Heat duty of the fuel gas stream, from 1700 °C to 120 °C, the heating of water from 50 °C to 185 °C and the evaporation of the water at 185 °C, which is the boiling point for water at 11 bar.

Stream	Heat duty
Fuel gas	1.51 MW
Heating	0.33 MW
Evaporation	1.15 MW

Figure C.1 shows the pinch analysis for the boiler. The graph shows that the minimum temperature difference is between the flue gas at 120 °C and the

liquid water at 50 °C, which is much higher than the minimum requirement of 10 °C. The two red lines do not touch due to rounding in the calculation and the use of an average specific heat for the heating stream.

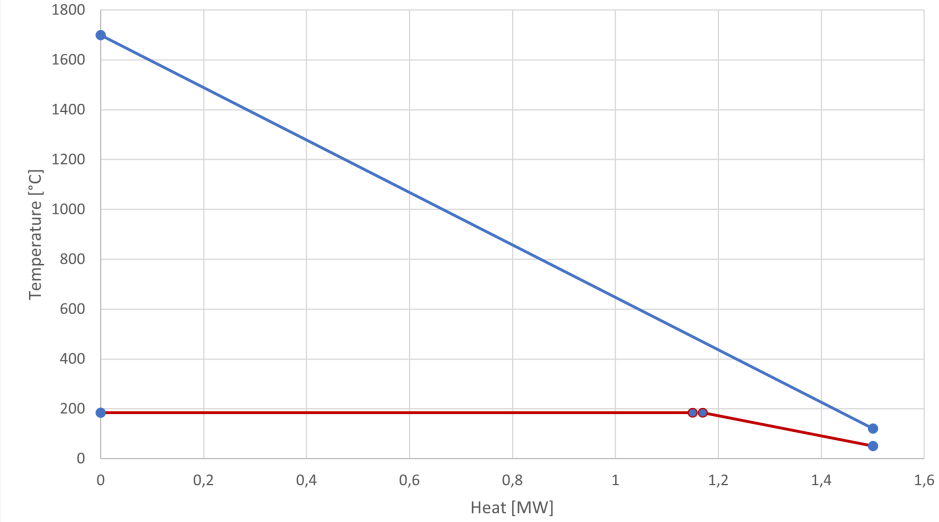

Figure C.1: Simple pinch analysis for the streams of the boiler. The blue line is the fuel gas stream, from 1700 °C to 120 °C. The red slope indicates the heating of water from 50 °C to 185 °C. The horizontal red line indicates the evaporation of the water at 185 °C, which is the boiling point for water at 11 bar.

Appendix D

Sizing and cost

D.1 Sizing calculations

This section will present the methods for sizing of the equipment. The method for the equipment in the base case, Alternative 1 and Alternative 2 will be presented.

D.1.1 Base case

The base case was investigated in a previous work[12]. The case is unchanged, except for the updated composition of the hydrogen production, which did not change the sizing or cost estimation for this case. The equipment that were sized in this case were a reactor, compressors, separators, heat exchangers and a storage tank. None of these equipment types were sized again in the work for this thesis. They are added to help the reader with understanding.

Compressor

The sizing of the compressors was performed in the Aspen Plus simulation. The required driver powers are shown in Table D.9.

Heat exchangers

The heat exchangers were primarily sized in the Aspen Plus simulation. Counter-current heat exchangers were used and the required area for the first four exchangers were estimated in the simulation. The estimated size

of the final two heat exchangers are shown in this section. All of the required exchanger areas are shown in Table D.11. An overall heat transfer coefficient, U, of 0.85 kW/m^{2}K was used for all the exchangers.

The required heat duty, Q, of the heat exchangers were 32.9 kW for HX105 and 33.8 kW for HX106. These values come from simulations of coolers in Aspen Plus, that cools the gas stream to the desired temperature. The required areas can be estimated from Equation D.1.1

$$Q = UA\Delta T_m \tag{D.1.1}$$

where A is the required area and ΔT_m is the logarithmic mean temperature difference.

The area was then calculated from Equation D.1.1. The required areas for HX105 and HX106 were found to be 0.74 m^2 and 0.76 m^2 respectively.

Separators

The separators were designed using the method given in section 10.9 in *Chemical Engineering Design* by Sinnott and Towler[25]. Parameters of the streams entering the separators, which are required for the calculation, are shown in Table D.1. These parameters come from the simulation in Aspen Plus.

Table D.1: Properties of the streams entering the separators.

Separator	Liquid density [kg/m^3]	Liquid flow [kg/h]	Vapor density [kg/m^3]	Vapor flow [kg/h]
S101	998.7	48.6	0.1	58.3
S102	998.7	5.4	0.3	52.9
S103	998.5	1.7	0.9	51.2
S104	998.0	0.5	2.9	50.7
S105	996.8	0.2	8.7	50.5
S106	994.4	0.1	24.6	50.5

The settling velocity, u_t, was calculated as follows

$$u_t = 0.07 \left(\frac{\rho_l - \rho_v}{\rho_v} \right)^{1/2} \tag{D.1.2}$$

where ρ_l is the liquid density and ρ_v is the vapor density. As a demister was not used, the settling velocity was multiplied by a factor of 0.15 to get the velocity, u_s, that was used in further calculations. For a vertical separator, the minimum allowable vessel diameter, D_v, is given by

$$D_v = \left(\frac{4V_v}{\pi u_s}\right)^{1/2} \tag{D.1.3}$$

where V_v is the volumetric flow rate of the vapor. The volumetric flow rate is calculated as follows

$$V[\mathrm{m}^2/\mathrm{s}] = \frac{\text{Mass flow rate[kg/h]}}{3600\mathrm{s/h} \cdot \rho[\mathrm{kg/m}^3]} \tag{D.1.4}$$

A liquid hold-up of two minutes was chosen. The required liquid volume is then given by

$$\text{Required liquid volume} = V_l \cdot 2\mathrm{min} \cdot 60\mathrm{s/min} \tag{D.1.5}$$

where V_l is the volumetric liquid flow rate. The required liquid height is then given as

$$h_l = \frac{\text{Required liquid volume}}{\pi \cdot D_v^2/4} \tag{D.1.6}$$

The total height of the vessel is the sum of the required liquid height, $D_v/2$ (minimum 0.6 m) and D_v (minimum 1 m). Since all of the liquid heights were small due to the low flow rates, the vessel height of the separators are all close to the minimum height, which is 1.6 m. The diameters varies from 0.44 m to 0.1 m.

As the sizing parameter for the cost estimation of separators is the shell mass, the wall thickness, t_w, is needed. This was calculated by Equation 13.41 from Sinnott and Towler. The equation specified by the ASME BPV Code (Sec. VIII D.1 Part UG-27) is given as

$$t_w = \frac{P_i D_i}{2SE - 1.2P_i} \tag{D.1.7}$$

where P_i is the internal pressure. The design pressure that was used is 10% higher than the operating pressure. D_i is the internal diameter. S is the maximum allowable stress for the material. The value for 304 stainless steel at 38 °C is 20.0 ksi and was obtained from Table 13.2 in Sinnott and Towler, based on ASME BPV Code Sec. VIII D.1. E is the welded joint efficiency. A value of 1 was used in the calculations.

The shell mass is the given by

$$\text{Shell mass} = \pi \cdot D \cdot H \cdot t_w \cdot \rho_{304ss} \tag{D.1.8}$$

where H is the height and ρ_{304ss} is the density of 304 stainless steel (= $8000\,\text{kg/m}^3$, from Table 7.2 in Sinnott and Towler). The shell masses of the separators are given in Table D.13.

Reactor

The volume of the reactor was assumed to be decided by the required water volume with the stated assumptions. The basis for the calculation is the yearly consumption of ash of 50000 tons. With 3500 operating hours, a mass flow of approximately 14 tons per hour is obtained. With the assumed ratio between water and ash of 1.4, 19.5 tons of water is required per hour. With a water density of $1000\,\text{kg/m}^3$, the volumetric flow of water is $19.5\,\text{m}^3\text{/h}$. An additional space of 10% was added to the volume and a residence time of three hours was used. The volume of the reactor is then

$$\begin{aligned}\text{Reactor volume} &= 19.5\,\text{m}^3\text{/h.} \cdot 1.1 \cdot 3\,\text{h} \\ &= 64.5\,\text{m}^3\end{aligned} \tag{D.1.9}$$

Storage tank

The storage tank was designed for being able to store one day's hydrogen production. The production is 50 kg/h with 14 operating hours per day. This gives a daily production of 700 kg. The density of the product stream, containing hydrogen, water and ammonia at 350 bar, was obtained from the simulation in Aspen Plus and had a value of $24.6\,\text{kg/m}^3$. The required volume of the tank is then obtained by dividing the daily production by the density of the stream.

$$\begin{aligned} \text{Required volume} &= \frac{700\,\text{kg}}{24.6\,\text{kg/m}^3} \\ &= 28.5\,\text{m}^3 \end{aligned} \tag{D.1.10}$$

Assuming a height/diameter ratio of 2, the diameter, D, was found to be 2.6 m and the height, h, to be 5.3 m using the formula for the volume of a cylinder as follows

$$V = \pi r^2 h \tag{D.1.11}$$

with the radius $r = D/2$. The wall thickness and shell mass was then estimated as described in the size estimation of the separators. The design pressure that was used was 385 bar. This gave a wall thickness of 0.44 m and a shell mass of 153 000 kg.

D.1.2 Scrubber

The diameter of the scrubbers were estimated by rewriting Equation D.1.12 as follows.

$$\dot{V} = A_c \cdot v \tag{D.1.12}$$

where $\dot{V}$ is the volume flow of the gas, A_c is the cross-sectional area of the scrubber and v is the gas velocity which is assumed to be 2 m/s. The cross-sectional area is given as

$$A = \frac{\pi \cdot D_s^2}{4} \tag{D.1.13}$$

where D_s is the inner diameter of the scrubber. By rewriting the equations, the diameter is found by

$$D_s = \sqrt{\frac{4 \cdot \dot{V}}{\pi \cdot v}} \tag{D.1.14}$$

As the volume flow of the gas varies depending on the pressure of the inlet gas flow, a diameter was calculated for each pressure. This diameter was

then used as a starting point for the sizing in Aspen Plus, using Aspen Process Economic Analyzer. Aspen Plus then gave a new diameter which were used for further calculation. Both the estimated and the diameter from Aspen are shown in Table D.2, together with the volumetric flow.

Table D.2: Volumetric flow for the inlet gas stream extracted from the Aspen Plus simulations. The estimated diameter, D_{est}, and the diameter given from the Aspen Plus simulation, D_{sim}, are also given.

	Vol flow	D_{est}	D_{sim}
1 bar	$0.1707\,\mathrm{m}^3/\mathrm{s}$	0.33 m	0.30 m
35 bar	$0.0049\,\mathrm{m}^3/\mathrm{s}$	0.06 m	0.15 m

The volume of both the packing and vessel is calculated as the volume of a cylinder using Equation D.1.15, with diameters from Table D.1.14 and heights from Table D.3 and D.4.

$$V = \frac{\pi}{4} \cdot D \cdot h_{cyl} \tag{D.1.15}$$

where D is the diameter and h_{cyl} is the height of the cylinder.

The diameter, height and volume of the packing and the vessel of the scrubbers are shown in Table D.3 and D.4. The heights were given by the Aspen Plus simulation by performing sizing calculations with Aspen Process Economic Analyzer (APEA) as described earlier. The heights for the packings given by APEA were smaller than expected. With an already high uncertainty, the packing heights were scaled up by a factor of 5 to be closer to expected values and ensure that the estimations would at least not be much smaller than the expected real life scenario. The increase in packing height was added to the vessel height exctracted from the simulation to get the new scaled up height. The following cost estimation showed that the scrubbers are a very small part of the total cost of Alternative 1, so even an upscaled, most likely too high estimate, would not make the scrubber cost significant.

The design pressure is chosen as 10% higher than the operating pressure. The wall thickness and shell mass are calculated as described for the separators under the base case. The data for the design of the scrubber vessels at 1 bar and 35 bar are shown in Table D.5.

Table D.3: Diameter, height and volume of the packing for the scrubbers at 1 bar and 35 bar. The height is the new, scale up height as described.

	Diameter	Height	Volume
1 bar	0.30 m	3.05 m	0.215 m^3
35 bar	0.15 m	3.05 m	0.054 m^3

Table D.4: Diameter, height and volume of the vessel of the scrubbers at 1 bar and 35 bar. The height is the new, scale up height as described.

	Diameter	Height	Volume
1 bar	0.30 m	7.32 m	0.517 m^3
35 bar	0.15 m	7.32 m	0.129 m^3

D.1.3 Boiler

The sizing of the boiler was performed in the Aspen Plus simulation. The duty, the heat production of the combustion, is shown in Table 4.8.

D.1.4 Pump

The sizing of the pump was performed in the Aspen Plus simulation. The flow and duty of the pump are shown in Table 4.9.

D.2 Cost estimation

This section will present the method of estimation the cost of the project. The method for the base case, Alternative 1 and Alternative 2 will be presented.

Equation 3.5.1 will be used for the cost estimation of all of the equipment, with the exception of the storage tank. This appendix will present the

Table D.5: Data for the design of the scrubber vessels.

	Volume	Design pressure	Wall thickness	Shell mass
1 bar	0.517 m^3	1.1 bar	0.0001 m	6.61 kg
35 bar	0.129 m^3	38.5 bar	0.0021 m	58.78 kg

cost parameters used in the estimation for all of the equipment. These parameters comes from Table 6.6 in Sinnott and Towler [25].

A cost index will be used to account for cost escalation. This is needed as the data from Sinnott and Towler will give cost estimations for Jan. 2007. The costs were estimated for Jun. 2021, as this was used in the earlier work. The Chemical Engineering Plant Cost Index (CEPCI) [32] was chosen. Table D.6 shows the Chemical Engineering Plant Cost Index used for the estimations.

Table D.6: CEPCI values [32] used for the cost estimation in this project. The values are averaged over the whole year, with the exception of 2007 and 2021.

Year	Index
2021 (Jun)	701.4
2018	603.1
2014	576.1
2011	585.7
2007 (Jan)	509.7

The costs were then adjusted with Equation D.2.1.

$$C_{\text{Jun 2021}} = C_{year} \cdot \frac{CI_{\text{Jun 2021}}}{CI_{year}} \tag{D.2.1}$$

where $C_{\text{Jun 2021}}$ is the new cost that have accounted for cost escalation. C_{year} is the cost for the initial year. CI is the CEPCI for the given year.

The costs including installation were estimated using installation factors proposed by Hand, Hand factors. The factors are described in section 6.3.3. in Sinnott and Towler. The Hand factors proposed for the equipment used in this project are given in Table D.7. The factors are from Table 6.3 in Sinnott and Towler.

The installed cost of the equipment can be estimated using Equation D.2.2.

$$C_{inst} = F_H \cdot C_e \tag{D.2.2}$$

where C_{inst} is the estimated cost for the installed equipment. F_H is the Hand factor of the equipment. C_e is the purchased equipment cost.

Table D.7: Table over Hand factors for estimating the installation cost of the equipment. The factors are from Table 6.3 in Sinnott and Towler [25].

Equipment type	Factor
Compressors	2.5
Fired heaters	2
Heat exchangers	4
Miscellaneous equipment	2.5
Pressure vessels	4
Pumps	4

For equipment that are in contact with water, as most of the equipment in this project, stainless steel is advised to be used. This will give an increase in the cost compared to carbon steel and will be accounted for. Some of the equipment are already estimated using stainless steel. The remaining equipment will have to be multiplied by a factor of 1.3, as of Table 6.5 in Sinnott and Towler.

D.2.1 Base case

As described for the base case in Appendix D.1, the cost estimation for the base case was performed in a previous work [12]. The calculations are added to help the reader with understanding.

The tables for the cost of the equipment of the base case are given in the sections below. The total cost for the equipment and the project overall are given in Table 4.13.

Compressors

The parameters for the cost estimation of the compressors are shown in Table D.8. The values are for reciprocating compressors with driver power [kW] as the unit for size, S.

As the compressor sizing parameters were below the lower bound, the constant A in the cost equation was scaled to get a more reasonable cost. The scaled parameter A_s that was used is given as

$$a_s = \frac{S}{S_{lb}} \cdot a \tag{D.2.3}$$

Table D.8: Parameters for the cost estimation of the compressors.

Parameter	Value
a	220 000
b	2300
n	0.75

where S is the size of the compressor and S_{lb} is the lower bound of the sizing parameter (=93 kW).

The required electricity for the compressors is found from the required duty of all the compressor, found in Table D.9 and the 3500 yearly operating hours.

$$\begin{aligned} El_{Comp} &= \text{Total compressor duty} \cdot \text{Operating hours} \\ &= 165.9\,\text{kW} \cdot 3500\,\text{h/year} \\ &= 580\,650\,\text{kW h} \approx 581\,000\,\text{kW h} \end{aligned} \tag{D.2.4}$$

To calculate the electricity cost, the required electricity was multiplied by the electricity price. The electricity price is obtained for industry except power-intensive industry from Statistics Norway (SSB) [33], with an exchange rate of 0.11 USD/NOK from DNB [34].

$$\begin{aligned} C_{El} &= \text{Electricity usage} \cdot \text{Electricity price} \\ &= 581\,000\,\text{kW h/year} \cdot 0.08\text{USD/kWh} \\ &= 46000\text{USD/year} \end{aligned} \tag{D.2.5}$$

Table D.9 shows the sizing parameter, power, and the cost with and without installation included for the compressors.

Heat exchangers

The parameters for the cost estimation of the heat exchangers are shown in Table D.10. The values are for a double pipe exchanger with area [m^2] as the unit for size, S.

Table D.9: Compressor duties and cost with and without installation.

Compressor	Power [kW]	Cost w/o inst. [USD]	Cost with inst. [USD]
C101	32.7	195000	488000
C102	32.4	192000	481000
C103	32.5	194000	484000
C104	33.1	196000	491000
C105	35.2	208000	520000
Total	165.9	985000	2464000

Table D.10: Parameters for the cost estimation of the heat exchangers.

Parameter	Value
a	1600
b	2100
n	1.0

Table D.11 shows the sizing parameter, required area, and costs for the heat exchangers. The overall heat transfer coefficient U is also included, with the value from the simulation in Aspen Plus.

Table D.11: Required heat exchanger areas and cost with and without installation.

Heat exchanger	U [kW/m^{2}K]	Area [m^2]	Cost w/o inst. [USD]	Cost with inst. [USD]
HX101	0.85	2.97	14000	49100
HX102	0.85	1.05	6800	23700
HX103	0.85	0.83	6000	20900
HX104	0.85	0.76	5800	20000
HX105	0.85	0.74	5600	19600
HX106	0.85	0.76	5700	20000
Total	-	7.11	43800	153300

Separators

The parameters for the cost estimation of the separators are shown in Table D.12. The values are for a vertical pressure vessel in 304 ss with shell mass [kg] as the unit for size, S.

Table D.12: Parameters for the cost estimation of the separators.

Parameter	Value
a	15000
b	68
n	0.85

Table D.13 shows the sizing parameter, shell mass, and the costs for the separators.

Table D.13: Separator shell mass and cost with and without installation.

Separator	Shell mass [kg]	Cost w/o inst. [USD]	Cost with inst. [USD]
S101	3.5	20900	83700
S102	5.8	21100	84200
S103	10.3	21300	85300
S104	18.2	21700	87000
S105	34.6	22500	90200
S106	74.9	24300	97200
Total	-	131900	527500

Reactor

The parameters for the cost estimation of the reactor are shown in Table D.14. The values are for a jacketed agitated reactor in 304 ss with volume [m^3] as the unit for size, S.

Table D.14: Parameters for the cost estimation of the reactor.

Parameter	Value
a	53000
b	28000
n	0.8

Table D.15 shows the sizing parameter, volume, and the cost of the reactor.

Table D.15: Required reactor volume and cost with and without installation.

Volume [m^3]	Cost w/o inst. [USD]	Cost with inst. [USD]
64.4	1152000	2881000

Storage tank

Due to the unreasonably high wall thickness, following shell mass and cost, the cost of the storage tank was estimated using an average of four alternative cost estimations at similar design pressures found in the open literature. Gracia et al. (2018)[46] presented an economic hypothesis where a cost of 353 EUR/kg was used. Using this to estimate the cost for this project with a daily production of 700 kg, an exchange rate of 1.13 USD/EUR[34] and adjusting for cost escalation using Equation D.2.1 with values from Table D.6, the cost is given by

$$C_{ST} = 353\text{EUR/kg} \cdot 700\,\text{kg} \cdot 1.13\text{USD/EUR} \cdot \frac{701.4}{603.1} = 325000\text{USD} \quad \text{(D.2.6)}$$

with C_{ST} being the cost for the storage tank.

Hua et al. (2011)[47] present a cost estimation using 15.4 USD/kWh. Hydrogen has an energy density of 33.3 kWh/kg. Using this, and accounting for cost escalation as mentioned above, the cost is given by

$$C_{ST} = 15.4\text{USD/kWh} \cdot 33.3\,\text{kWh/kg} \cdot 700\,\text{kg} \cdot \frac{701.4}{585.7} = 430000\text{USD} \quad \text{(D.2.7)}$$

Hwang et al. (2014)[48] used a similiar estimation as Hua et al., but with a factor of 16 USD/kWh instead. Cost escalation was accounted for the same way as above and the cost is given by

$$C_{ST} = 16\text{USD/kWh} \cdot 33.3\,\text{kWh/kg} \cdot 700\,\text{kg} \cdot \frac{701.4}{576.1} = 454000\text{USD} \quad \text{(D.2.8)}$$

Paster et al. (2011)[49] found the cost to be 860 USD/kg. Using this estimate and accounting for cost escalation, the cost is given by

$$C_{ST} = 860\text{USD/kg} \cdot 700\,\text{kg} \cdot \frac{701.4}{585.7} = 721000\text{USD} \tag{D.2.9}$$

Since there is much uncertainty in how scaleable these methods are to this project, an average was used for the cost estimation. The average cost for the storage tank, $C_{ST,av}$ is given by

$$\begin{aligned} C_{ST,av} &= \frac{325000\text{USD} + 430000\text{USD} + 454000\text{USD} + 721000\text{USD}}{4} \\ &= 482000\text{USD} \end{aligned} \tag{D.2.10}$$

It is not clear if installation was included for the cost estimations in the literature, so a cost including installation is estimated using the factor for a pressure vessel from Table D.7.

$$C_{installed,ST,av} = 4 \cdot 482000\text{USD} = 1930000\text{USD} \tag{D.2.11}$$

In addition to this, an alternative estimation of the cost of the storage tank using a scaled down wall thickness of 44 mm (10% of original) was done. This may be a reasonable thickness when looking at other articles which gave thicknesses from 5 to 20 mm [50] [51] for high pressure vessels, but using much smaller volumes. The shell mass was then 10% of the shell mass calculation for the storage tank shown in Appendix D.1. This gave a cost of 358000 USD without installation, using Equation 3.5.1 and parameters for a vertical pressure vessel in 304 ss as shown in Table D.12. The cost was 1431000 USD with installation, which is relatively close to the calculated average cost from the articles.

Table D.16 shows the estimated volume and the cost of the storage tank.

Table D.16: Volume and costs with and without installation for the storage tank.

Volume [m^3]	Cost w/o inst. [USD]	Cost with inst. [USD]
28.5	480000	1930000

D.2.2 Alternative 1: Fuel cells

Alternative 1 is as described the base case with the addition of a scrubber. Thus, the total cost of the alternative is the sum of the cost of the base case and the cost of the scrubber. The total cost of the alternative is shown in Table 4.16.

Scrubber

The cost of the packing of the scrubber was estimated using data for ceramic intalox saddles, shown in Table D.17. The sizing parameter S for the packing is the packing volume in m^3. The cost of the packing is shown in Table 4.15. There is no installation cost for the packing.

Table D.17: Parameters for the cost estimation of the packing.

Parameter	Value
a	0
b	1800
n	1.0

The cost of the scrubber vessel was estimated using data for a vertical pressure vessel in 304 ss, shown in Table D.18. The sizing parameter S for the vessel is the shell mass in kg. The cost of the vessel is shown in Table 4.16.

Table D.18: Parameters for the cost estimation of the scrubber vessel.

Parameter	Value
a	15000
b	68
n	0.85

The total cost of the scrubber is the sum of the cost of packing and the cost of the vessel. The total cost of the scrubber is shown in Table 4.16.

D.2.3 Alternative 2: Process heat production

The cost of Alternative 2 is based on the costs of the boiler and the pump for the steam producing loop. The total cost of the alternative is shown in Table 4.18.

Boiler

The cost of the boiler was estimated using data for a cylindrical furnace, shown in Table D.19. The size parameter S is the duty of the furnace in MW. The estimated cost is shown in Table 4.18.

Table D.19: Parameters for the cost estimation of the boiler.

Parameter	Value
a	68500
b	93000
n	0.8

Heat exchanger

As described in Chapter 3, the heat exchanger is not included in the cost estimation for Alternative 2.

Pump

The cost of the pump was estimated using data for a single stage centrifugal pump, shown in Table D.20. The size parameter S of the estimation is the flow in L/s. The estimated cost is shown in Table 4.18.

Table D.20: Parameters for the cost estimation of the pump.

Parameter	Value
a	6900
b	206
n	0.9

Appendix E

Simulation flow sheets

E.1 Base case

Figure E.1 shows the flow sheet of the Aspen Plus simulation for the base case.

E.2 Scrubber

Figure E.3 shows the flow sheet of the Aspen Plus simulation for the scrubbers.

E.3 Alternative 1: Fuel cells

Figure E.3 shows the flow sheet of the Aspen Plus simulation for Alternative 1.

E.4 Alternative 2: Process heat production

Figure E.4 shows the flow sheet of the Aspen Plus simulation for Alternative 2.

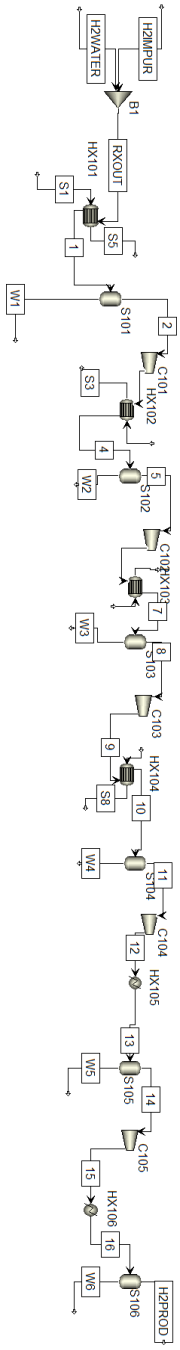

Figure E.1: Base case.

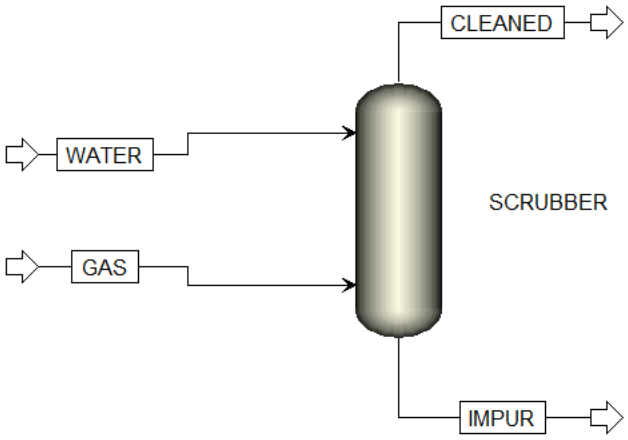

Figure E.2: Simulation flow sheet of the scrubbers from Aspen Plus. The flow sheet is the same for all of the scrubber simulations.

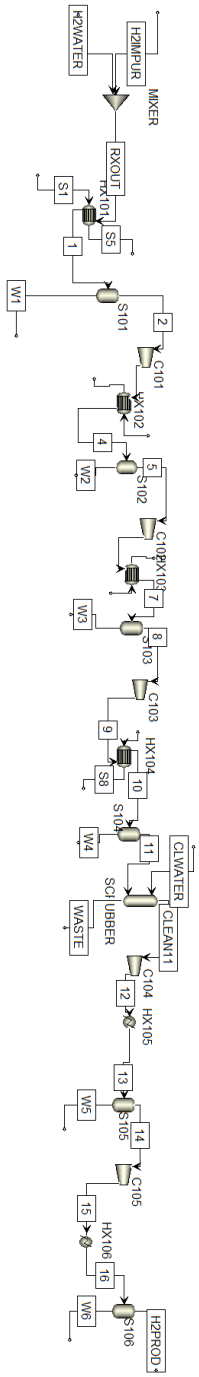

Figure E.3: Simulation flow sheet of Alternative 1 from Aspen Plus.

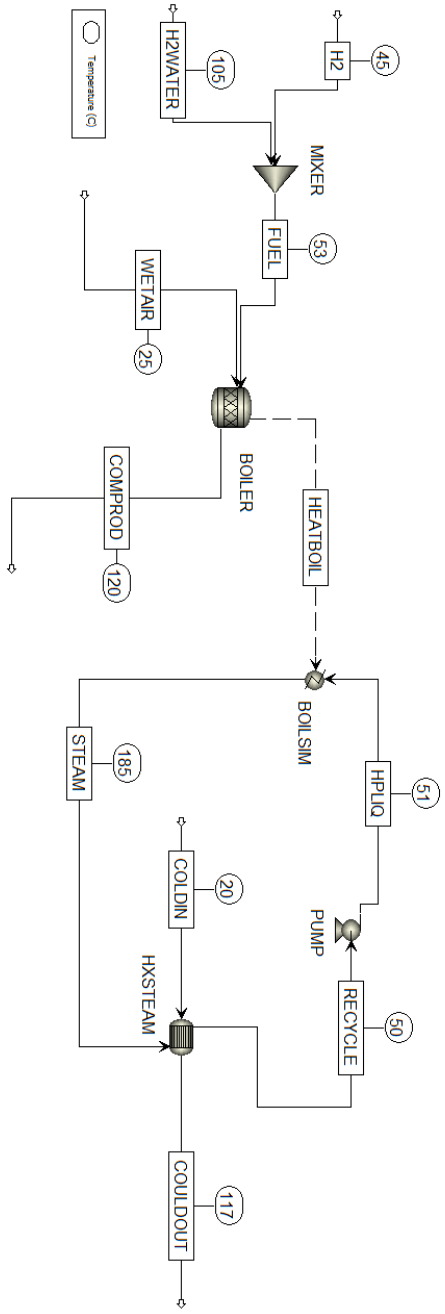

Figure E.4: Simulation flow sheet of Alternative 2 from Aspen Plus.

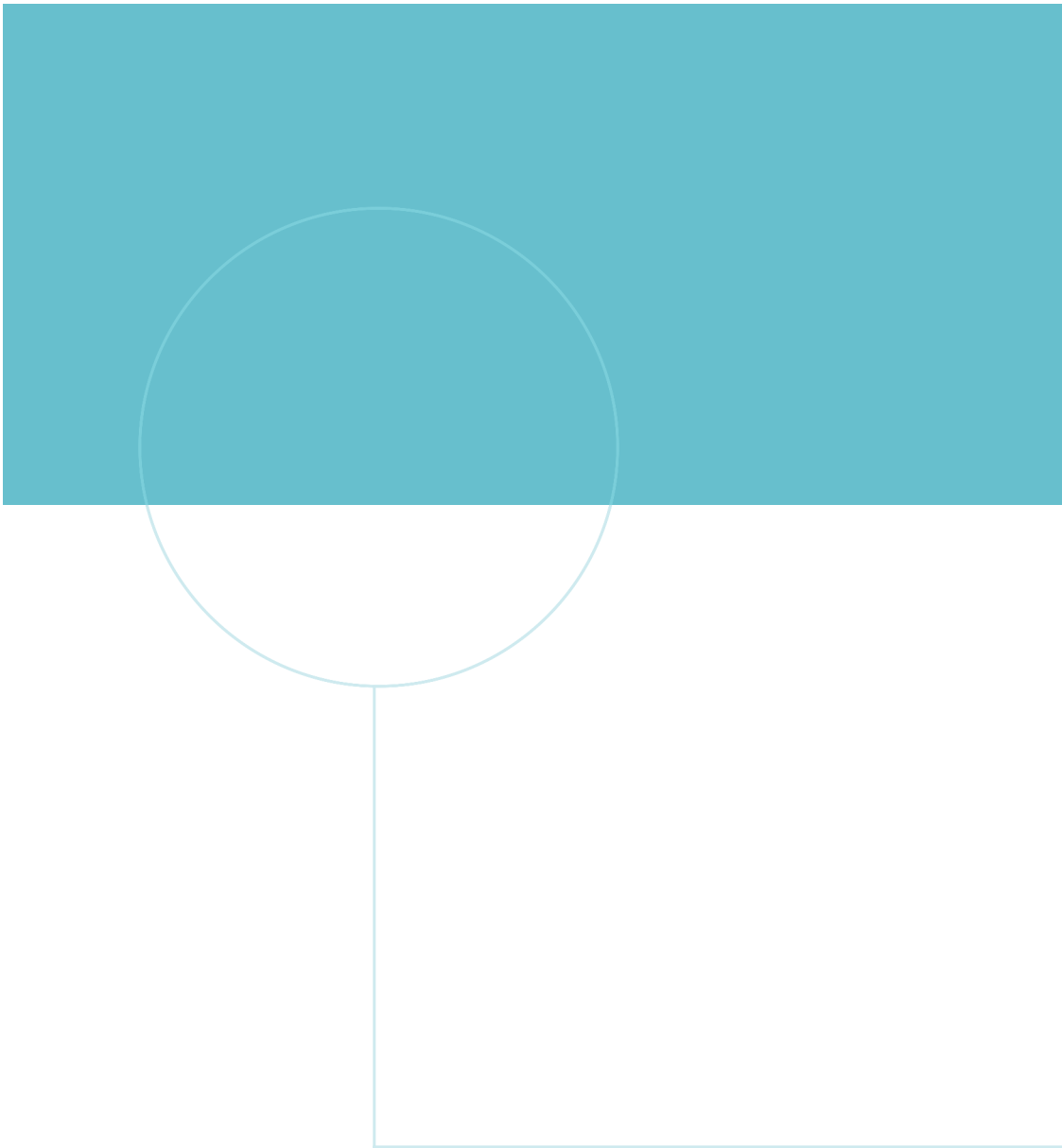

NTNU

Norwegian University of
Science and Technology